金国钧

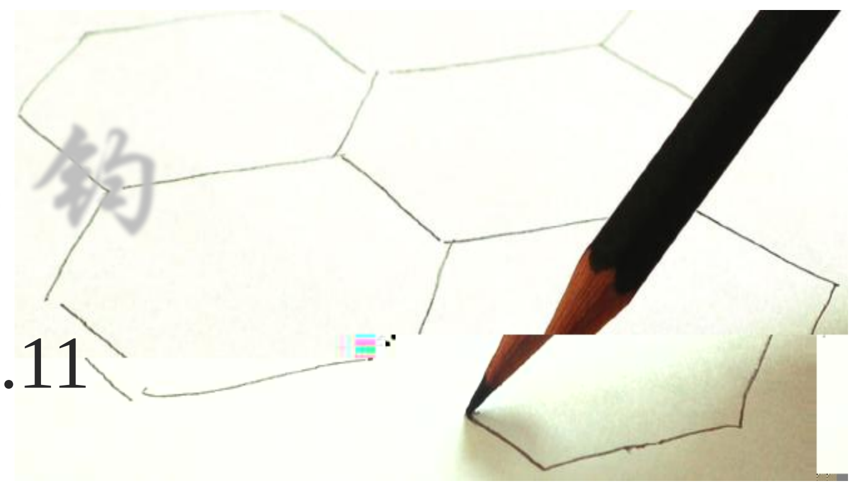

2015.6.11

Emergence of graphene

Electric Field Effect in Atomically Thin Carbon Films

Novoselov et al., **Science 306, 666 (2004)**

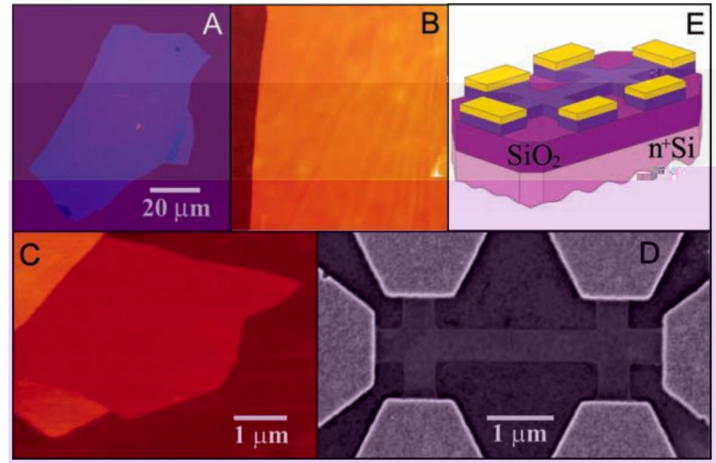

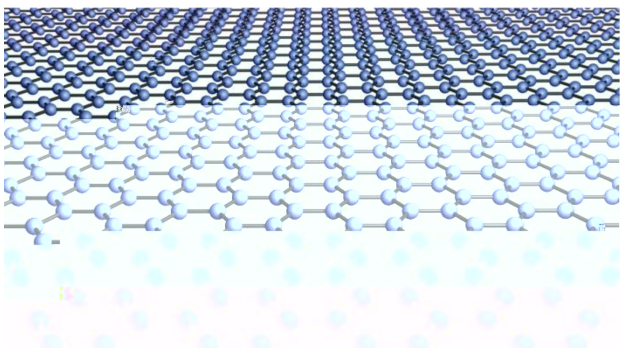

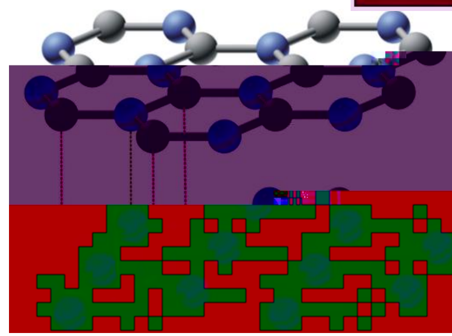

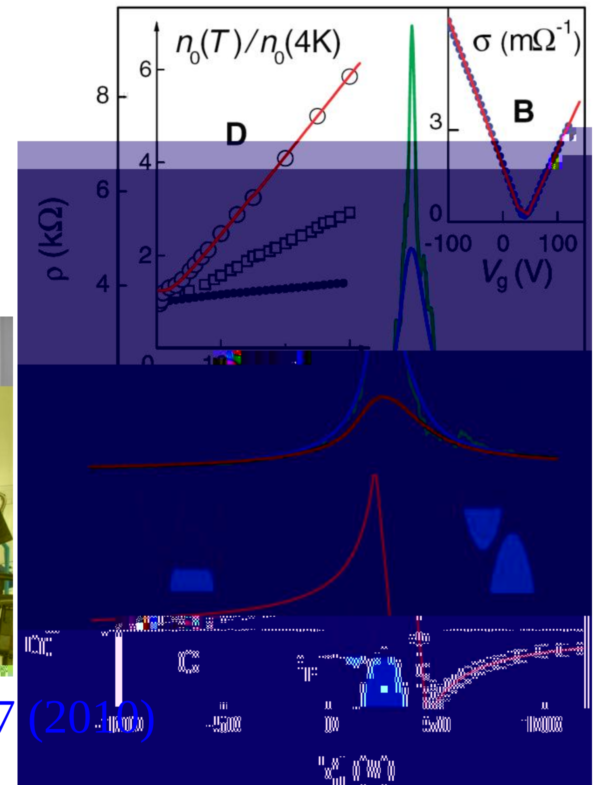

Graphene: Materials in the Flatland Novoselov, RMP 83, 837 (2010)

Carbon Wonderland

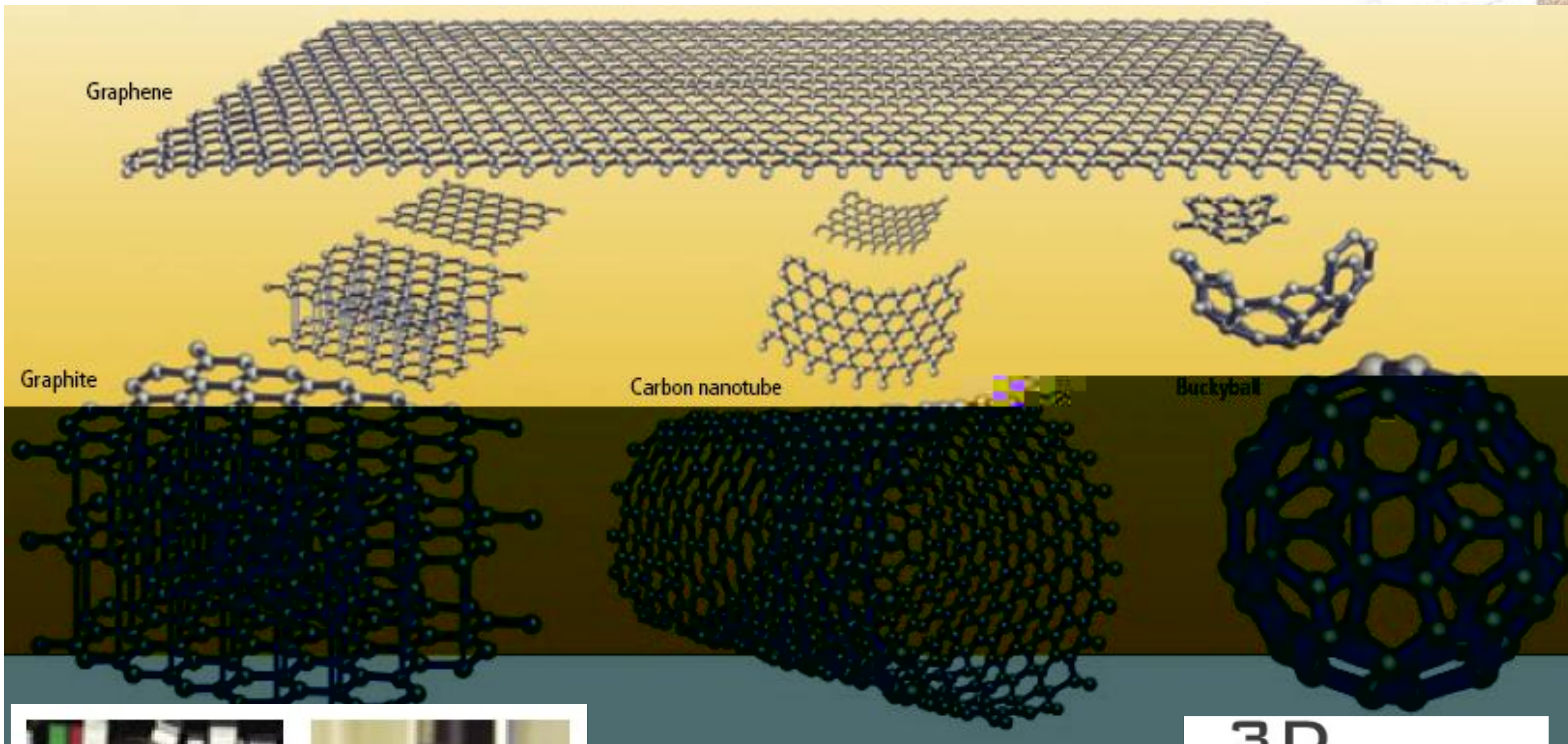


Geim(Manchester) Kim (Columbia)

A. K. Geim and P. Kim,
Sci. Am. April, 90 (2008)

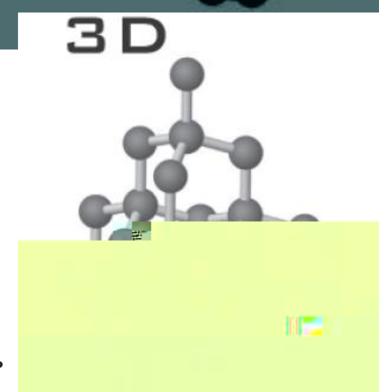

Ultrathin Epitaxial Graphite: …

C. Berger et al., J. Phys. Chem. B 108, 19912 (2004)

Geim and MacDonald, Phys. Today, Aug. 35 (2007)

Graphene: Exploring carbon flatland

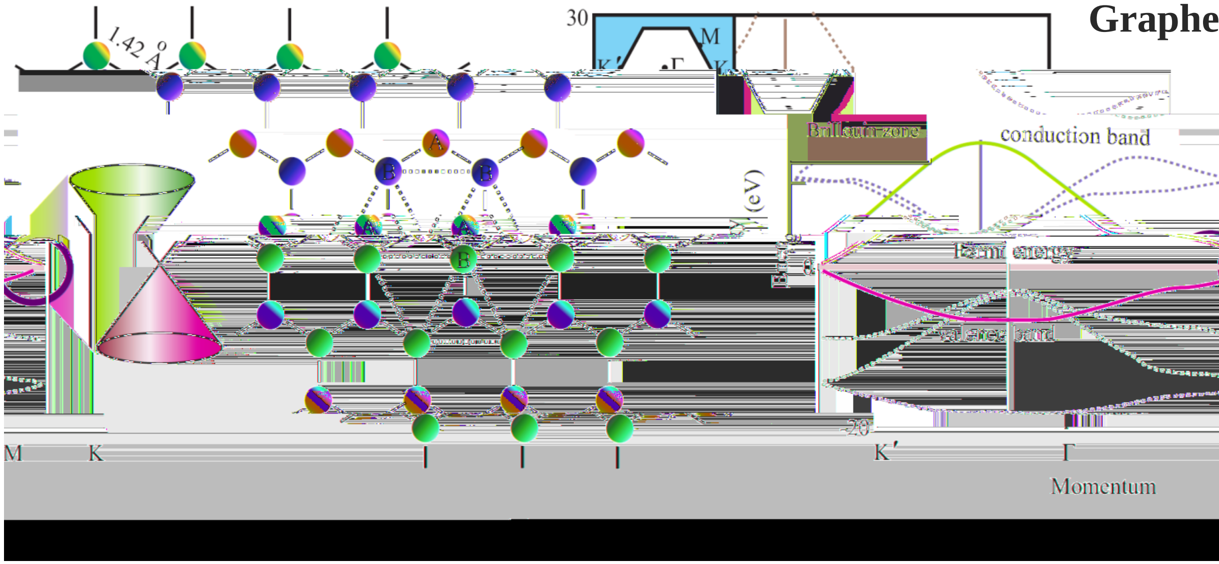

Dirac Fermi

$$\mathcal{H} = v_{\rm F}\, p \begin{pmatrix} 0 & e^{i\varphi(p)} \\ e^{-i\varphi(p)} & 0 \end{pmatrix}$$

Hall 底

Novoselov et al.,

Nature **438**, 197 (2005)

$$E_N = \mathrm{sgn}(N)\sqrt{2e\hbar v_{\rm F}^2 \,|\,N\,|\,B}$$

$$\sigma_{xy} = \pm 4(N+1/2)e^2/h$$

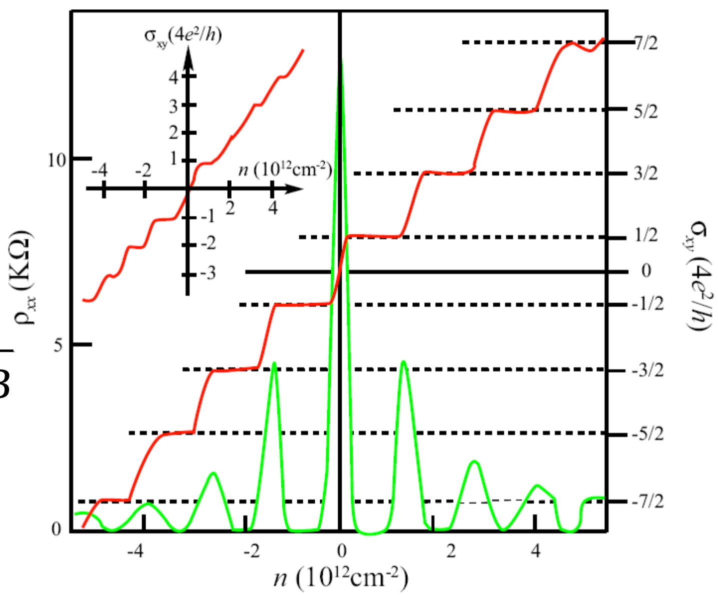

$$\mathcal{H} = \frac{p^2}{2m}$$

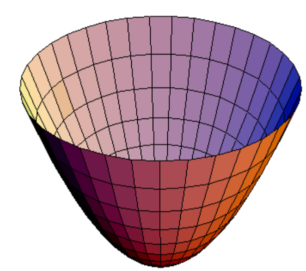

C. Zhang and G. Jin, JPCM **25**, 425604 (2013).

C. Zhang and G. Jin, APL **103**, 202111 (2013).

1. Background: Physical picture of excitons

a quasiparticle = an electron in conduction band
+ a hole in valence band with Coulomb interaction

$$\left[-\frac{\hbar^2\nabla_{\mathrm{e}}^2}{2m_{\mathrm{e}}}-\frac{\hbar^2\nabla_{\mathrm{h}}^2}{2m_{\mathrm{h}}}-\frac{e^2}{\epsilon|\boldsymbol{r}_{\mathrm{e}}-\boldsymbol{r}_{\mathrm{h}}|}\right]\Phi(\boldsymbol{r}_{\mathrm{e}},\boldsymbol{r}_{\mathrm{h}})=E\Phi(\boldsymbol{r}_{\mathrm{e}},\boldsymbol{r}_{\mathrm{h}})$$

play important role in the optical properties of semiconductors

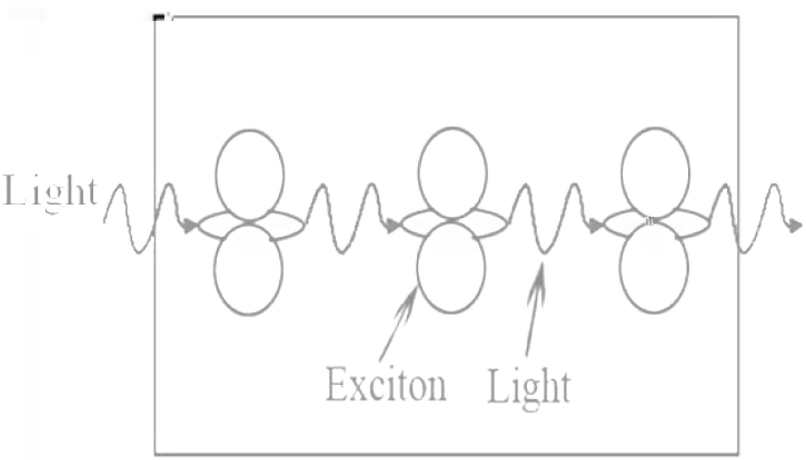

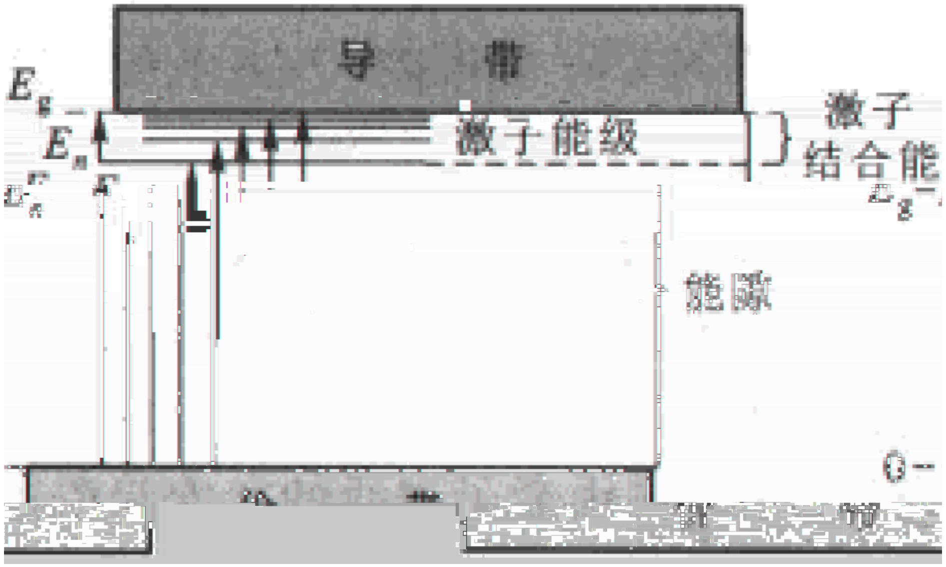

1. Background: Exciton condensation

proposed by Keldysh and Kopaev in1964 and studied by Soviet physicists

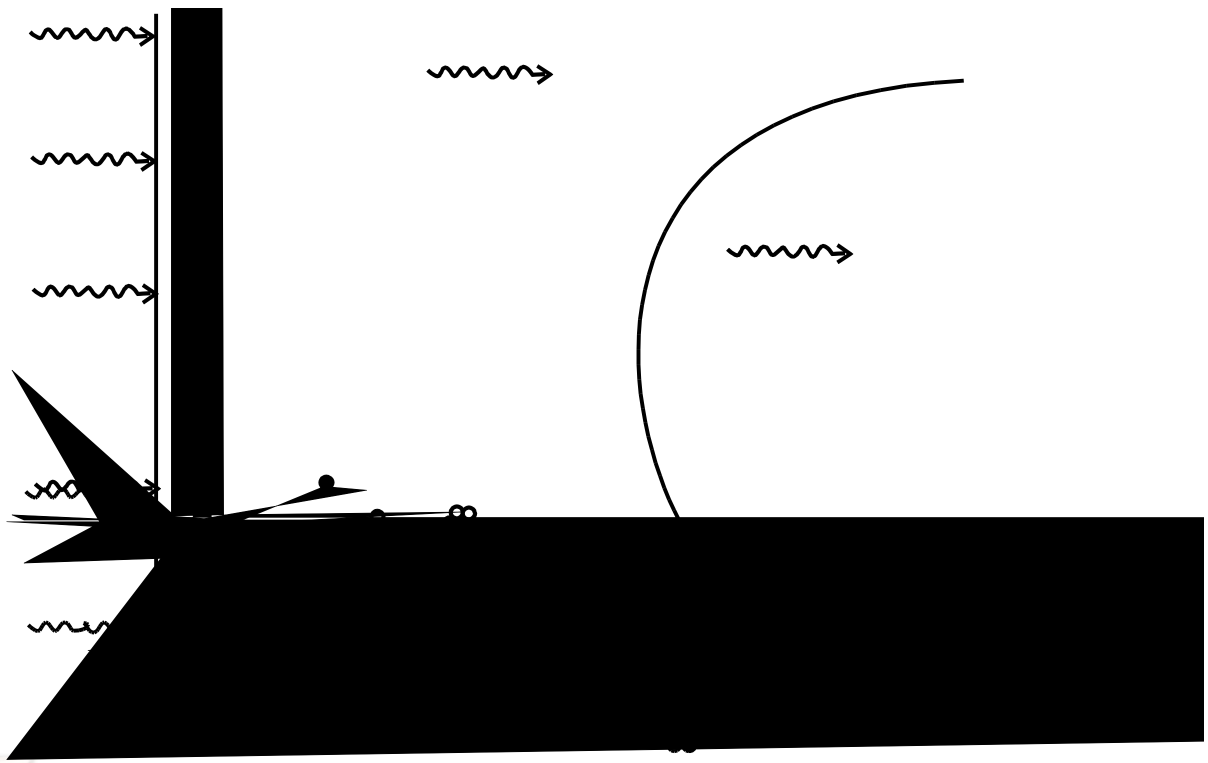

Electron-Hole

1. Background; Excitons in double quantum wells

LETTER Nature **483**, 584 (2012)

doi:10.1038/nature10903

Spontaneous coherence in a cold exciton gas

A. A. High[1], J. R. Leonard[1], A. T. Hammack[1], M. M. Fogler[1], L. V. Butov[1], A. V. Kavokin[2,3], K. L. Campman[4] & A. C. Gossard[4]

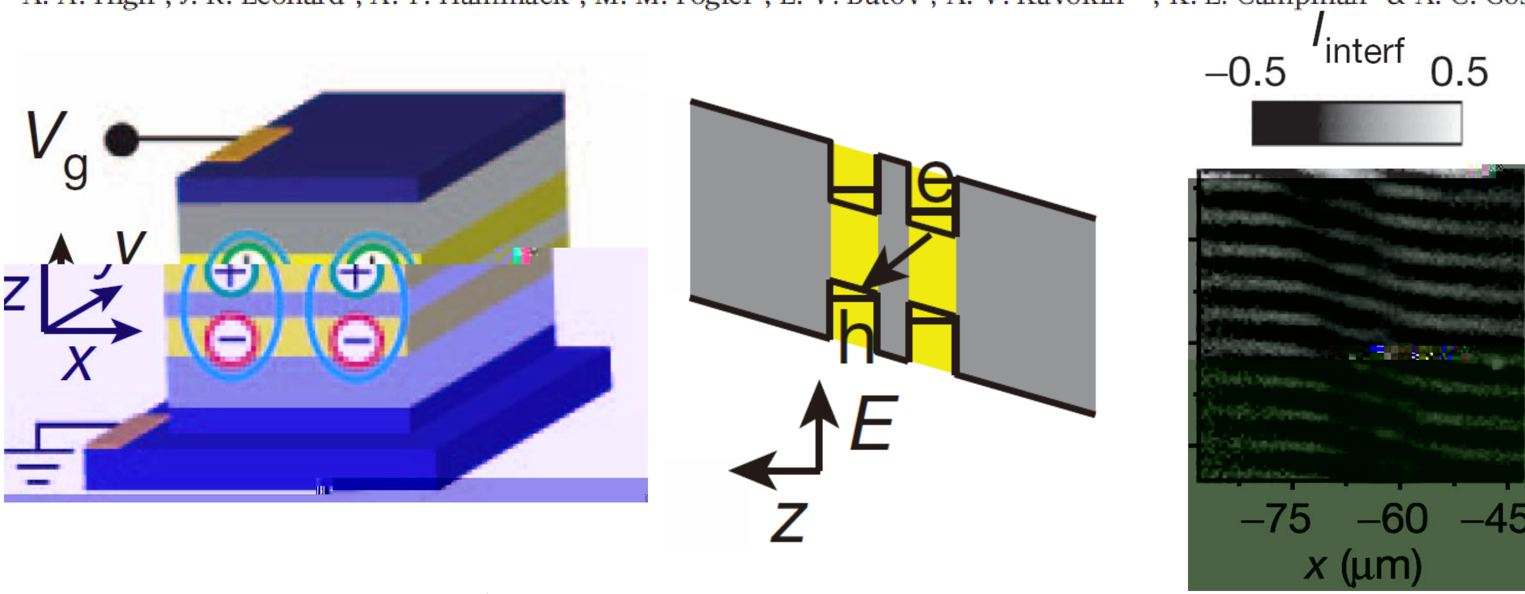

兴

左 反

Graphene

2. Exciton condensation in graphene bilayer:

Previousur research

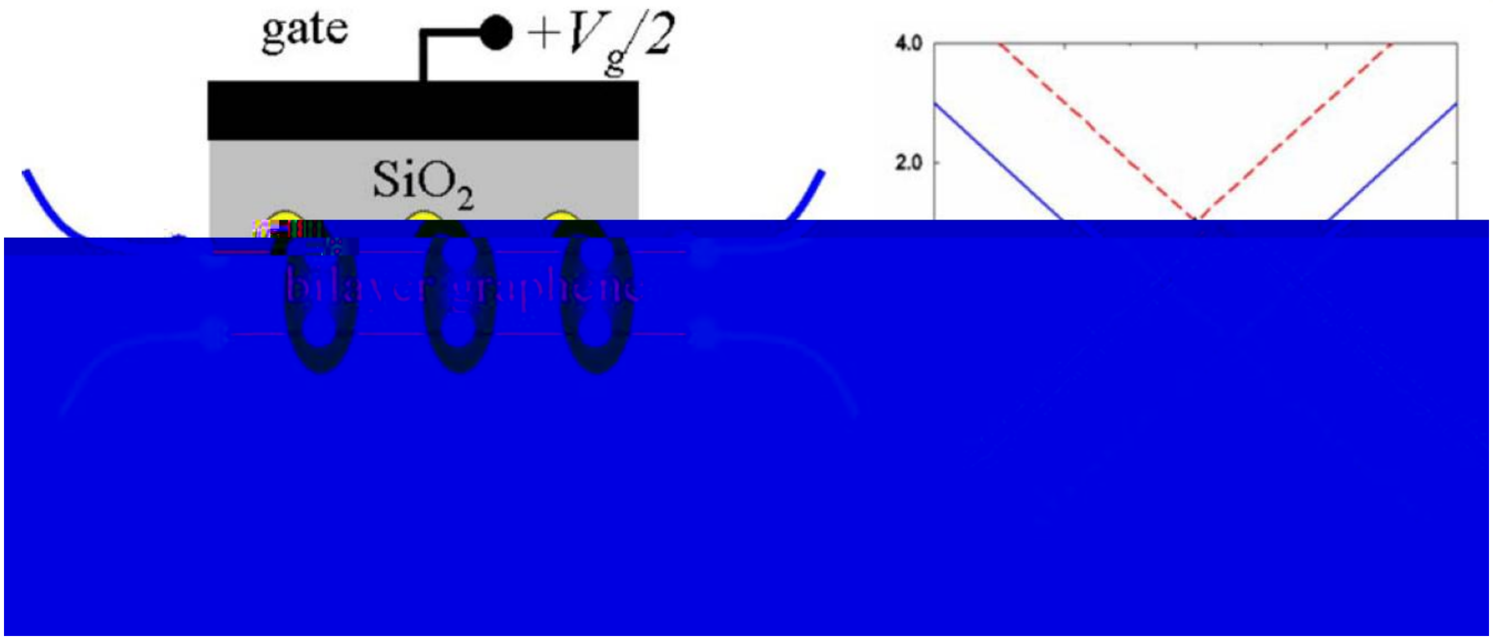

Fermi 兴 兴

C.-H. Zhang and Y. N. Joglekar, PRB **77**, 233405 (2008)

H. Min, R. Bistritzer, J. J. Su, and A. H. MacDonald, PRB **78**, 121401(R) (2008)

indicate possible room-temperature superfluidity

2. Exciton condensation in graphene bilayer:

Our considerations

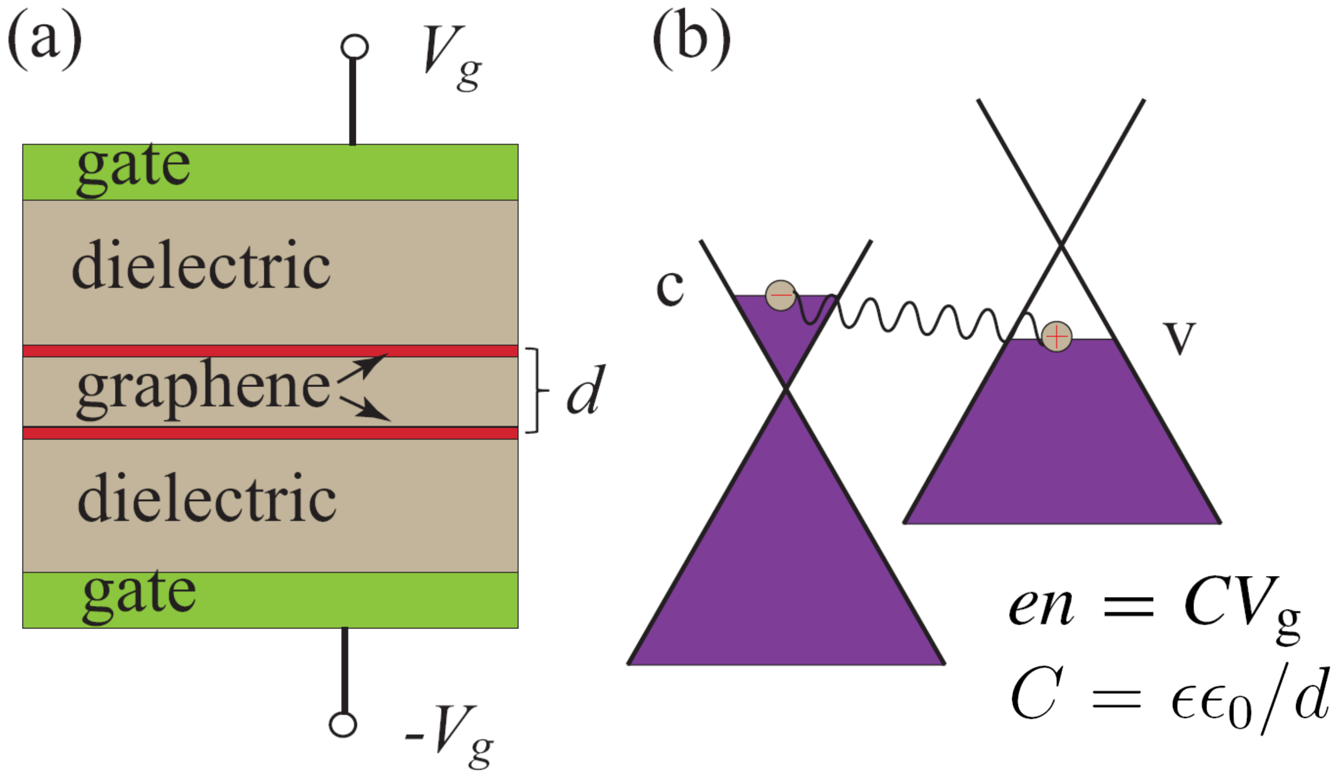

(a) 反 .

. (b) Fermi c v 下

2. Exciton condensation in graphene bilayer:

Formulation

$$\mathcal{H} = \sum_{\boldsymbol{k}} \left[(\hbar v_F k - eV_g) a^\dagger_{\mathrm{c}\boldsymbol{k}} a_{\mathrm{c}\boldsymbol{k}} + (-\hbar v_F k + eV_g) a^\dagger_{\mathrm{v}\boldsymbol{k}} a_{\mathrm{v}\boldsymbol{k}} \right]$$

$$+ \frac{1}{2} \sum_{\boldsymbol{k}\boldsymbol{k}'\boldsymbol{q}} [U^{\mathrm{ee}}_{\boldsymbol{q}} a^\dagger_{\mathrm{c},\boldsymbol{k}+\boldsymbol{q}} a^\dagger_{\mathrm{c},\boldsymbol{k}'-\boldsymbol{q}} a_{\mathrm{c}\boldsymbol{k}'} a_{\mathrm{c}\boldsymbol{k}} + U^{\mathrm{hh}}_{\boldsymbol{q}} a_{\mathrm{v},\boldsymbol{k}+\boldsymbol{q}}$$

$$\times a_{\mathrm{v},\boldsymbol{k}'-\boldsymbol{q}} a^\dagger_{\mathrm{v}\boldsymbol{k}'} a^\dagger_{\mathrm{v}\boldsymbol{k}} - 2U^{\mathrm{eh}}_{\boldsymbol{q}} a^\dagger_{\mathrm{c},\boldsymbol{k}+\boldsymbol{q}} a_{\mathrm{v},\boldsymbol{k}'-\boldsymbol{q}} a^\dagger_{\mathrm{v}\boldsymbol{k}'} a_{\mathrm{c}\boldsymbol{k}}]$$

Mean field treatment　　BCS like theory

Broken symmetry　　condensed phase to appear

2. Exciton condensation in graphene bilayer:

A set of coupled equations

$$E_+(k) = \hbar v_{\mathrm{F}} k - eV_{\mathrm{g}} + \frac{2\pi e^2 nd}{\epsilon} - \sum_{k'} U^{\mathrm{ee}}_{\boldsymbol{k}'-\boldsymbol{k}}[|v_{k'}|^2 + (|u_{k'}|^2 - |v_{k'}|^2) f(\varepsilon(k'))],$$

$$\Delta(k) = \frac{1}{2}\sum_{\boldsymbol{k}'} U^{\mathrm{eh}}_{\boldsymbol{k}'-\boldsymbol{k}} \frac{\Delta(k')}{\varepsilon(k')}\left[1 - 2f(\varepsilon(k'))\right],$$

$$\varepsilon(k) = \sqrt{E_+(k)^2 + \Delta(k)^2},$$

$$n = 4\sum_k \left[|v_k|^2 + (|u_k|^2 - |v_k|^2) f(\varepsilon(k))\right],$$

$$|v_k|^2 = 1 - |u_k|^2 = [1 - E_+(k)/\varepsilon(k)]/2$$

They could be solved self-consistently

2. Exciton condensation in graphene bilayer:

Condensation at zero temperature

$$\beta = e^2/(\epsilon \hbar v_{\mathrm{F}})$$

$$r_{\mathrm{s}} = 1/\sqrt{\pi n}$$

$$\chi(V_{\mathrm{g}}) = \frac{1}{2\pi}\int \left[\left(\frac{\mathrm{d}u_k}{\mathrm{d}V_{\mathrm{g}}}\right)^2 + \left(\frac{\mathrm{d}v_k}{\mathrm{d}V_{\mathrm{g}}}\right)^2\right] k\,\mathrm{d}k$$

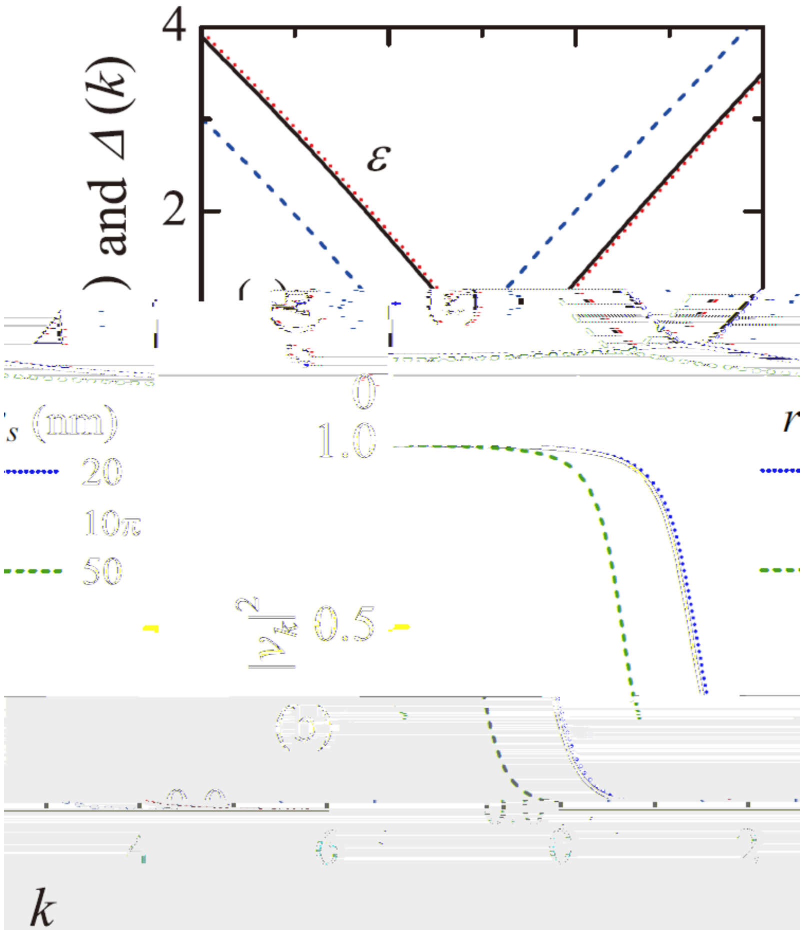

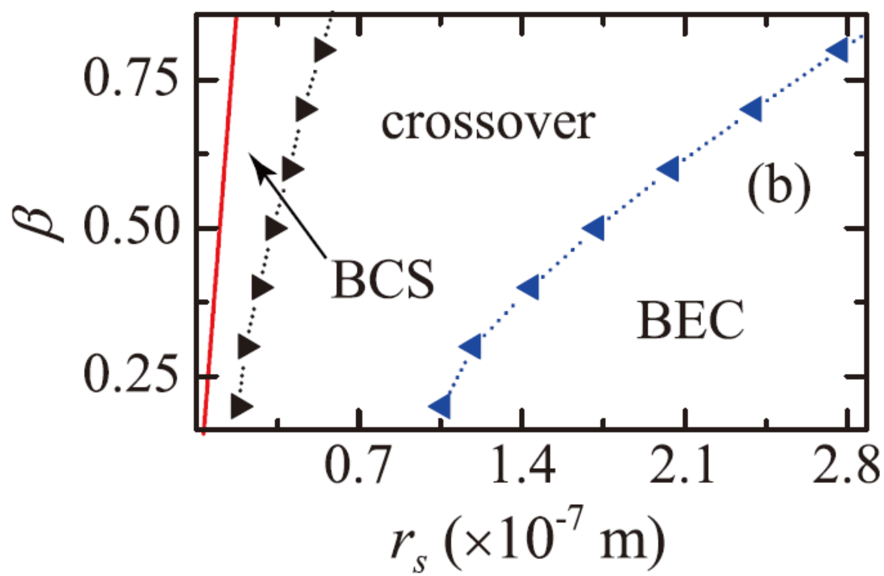

$$k_{\mathrm{m}} \approx \frac{1 - 2d\beta/r_{\mathrm{s}} \ldots}{r_{\mathrm{s}} k_u (1 - 2 \ldots}$$

$$\frac{d}{r_{\mathrm{s}}} < \frac{1}{2\beta}$$

2. Exciton condensation in graphene bilayer:

Superfluidity at finite temperature $(0 < T < T_C)$

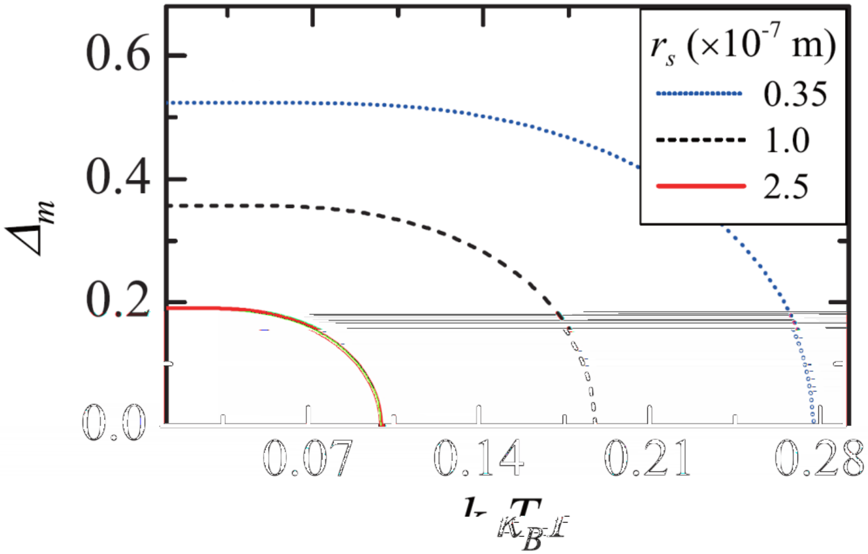

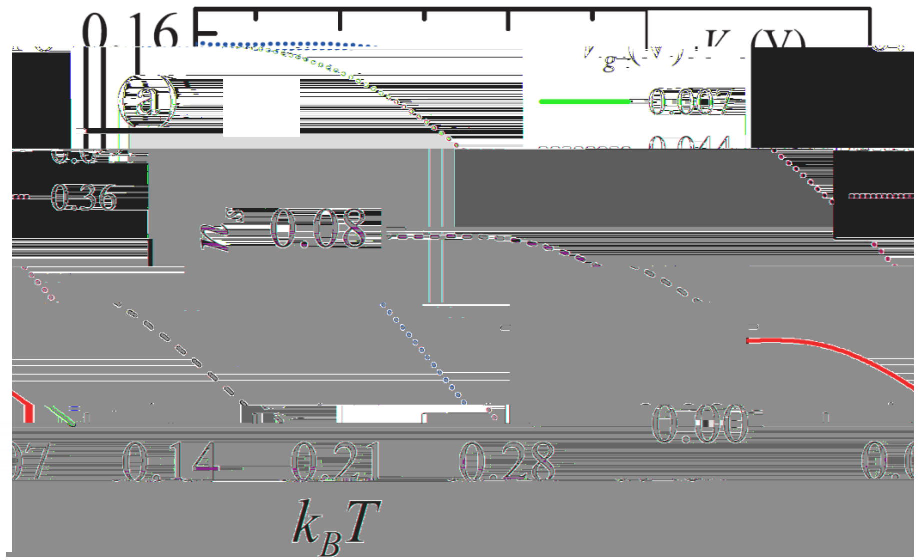

[redacted] as for conventional superconductor

$$n_{\mathrm{s}} \approx \frac{\hbar^2 v_{\mathrm{F}}^2}{16\pi k_{\mathrm{B}} T} \int \left(\mathrm{sech}^2 \frac{E_+(k)}{2k_{\mathrm{B}} T} - \mathrm{sech}^2 \frac{\varepsilon(k)}{2k_{\mathrm{B}} T} \right) k \, \mathrm{d}k$$

3. Thermal Josephson effect in graphene bilayer:

Previous studies

K. Maki and A. Griffin, PRL **15**, 921 (1965) Entropy transport between two superconductors by electron tunneling,

LETTER Nature **492**, 401 (2012)

doi:10.1038/nature1170

The Josephson heat interferometer

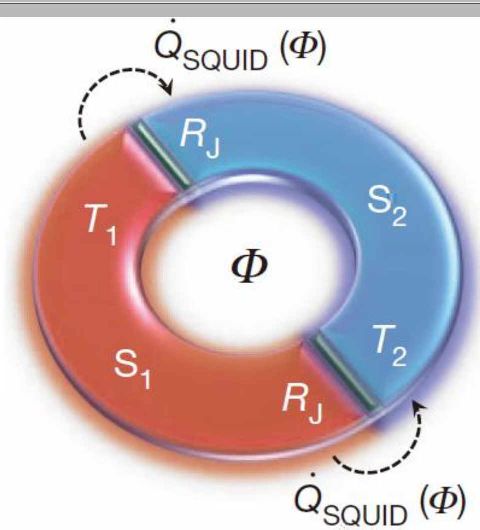

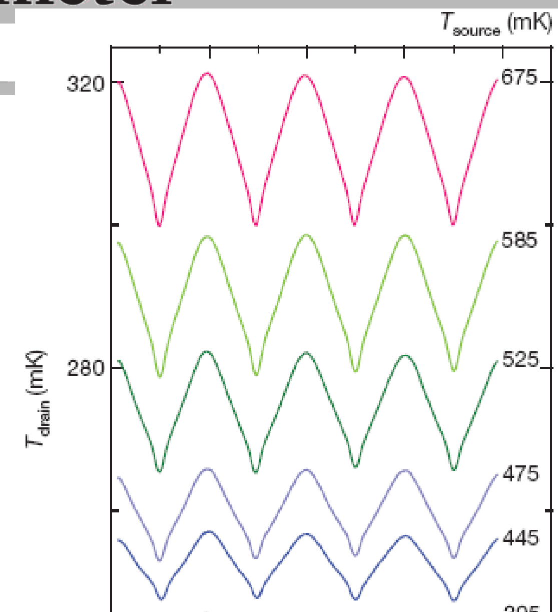

$$\dot{Q}_{SQUID}(\Phi) = 2\dot{Q}_{qp} - 2\dot{Q}_{int}\left|\cos\left(\frac{\pi\Phi}{\Phi_0}\right)\right|$$

phase-dependent thermal transport

3. Thermal Josephson effect in graphene bilayers:

Our considerations

assume T_L T_R

Josephson (1940-)

$$I = I_c \sin \Delta\phi$$

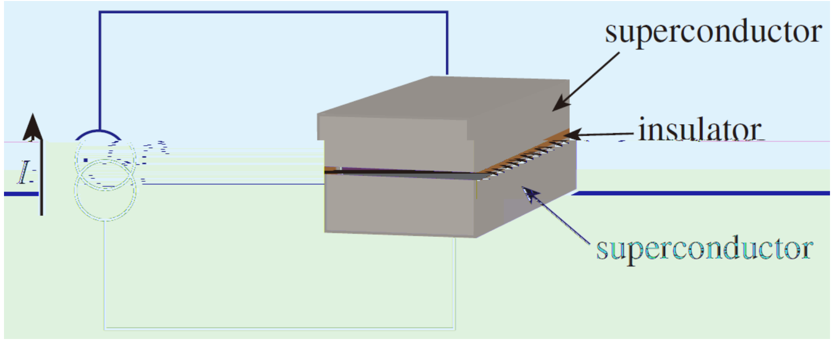

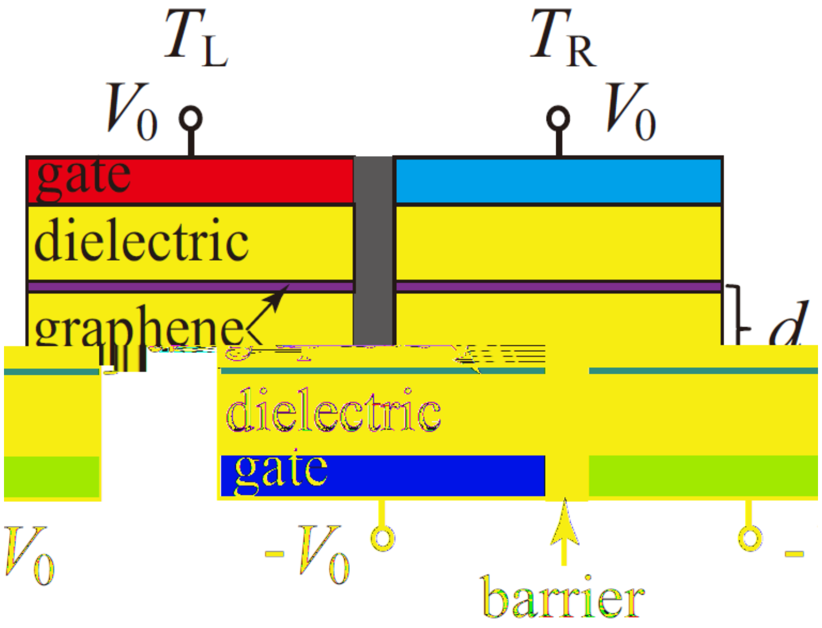

Josephson

.

d

B. D. Josephson, Phys. Lett. **1**, 251 (1962)

3. Thermal Josephson effect in graphene bilayers:

Formulation

ignore the intra-plane interactions

$$\mathcal{H} = \sum_{jk}\Big[(\hbar v_{\mathrm{F}}k - V_0)a^{\dagger}_{j\mathrm{c}\boldsymbol{k}}a_{j\mathrm{c}\boldsymbol{k}} + (-\hbar v_{\mathrm{F}}k + V_0)a^{\dagger}_{j\mathrm{v}\boldsymbol{k}}a_{j\mathrm{v}\boldsymbol{k}}\Big]$$

$$- \sum_{jkk'q} U_{\boldsymbol{q}}a^{\dagger}_{j\mathrm{c}\boldsymbol{k}+\boldsymbol{q}}a_{j\mathrm{v}\boldsymbol{k}'-\boldsymbol{q}}a^{\dagger}_{j\mathrm{v}\boldsymbol{k}'}a_{j\mathrm{c}\boldsymbol{k}}$$

$$+ \sum_{kk'}\Gamma_{\boldsymbol{kk}'}\Big(a^{\dagger}_{\mathrm{Lc}\boldsymbol{k}}a_{\mathrm{Rc}\boldsymbol{k}'} + a^{\dagger}_{\mathrm{Lv}\boldsymbol{k}}a_{\mathrm{Rv}\boldsymbol{k}'} + a^{\dagger}_{\mathrm{Rc}\boldsymbol{k}'}a_{\mathrm{Lc}\boldsymbol{k}} + a^{\dagger}_{\mathrm{Rv}\boldsymbol{k}'}a_{\mathrm{Lv}\boldsymbol{k}}\Big)$$

but add the inter-bilayer tunneling

By using equation of motion, thermal current is

$$I_{\mathrm{Q}} = I_{\mathrm{qp}} + I_{\mathrm{in}}$$

$\pm$ represents $\hbar v_{\mathrm{F}}k$ V_0 and the other

$$I_{\mathrm{qp}} = \frac{32|\Gamma|^2}{\pi(\hbar v_{\mathrm{F}})^2}\int_0^{+\infty}(V_0 \pm \sqrt{\varepsilon^2 - \Delta_{\mathrm{L}}^2})\left[f_{\mathrm{L}}(\varepsilon) - f_{\mathrm{R}}(\varepsilon)\right]\frac{\varepsilon^2}{\sqrt{\varepsilon^2 - \Delta_{\mathrm{L}}^2}}kdk$$

$$I_{\mathrm{in}} = -\frac{32|\Gamma|^2}{\pi(\hbar v_{\mathrm{F}})^2}\cos\varphi\int_0^{+\infty}(V_0 \pm \sqrt{\varepsilon^2 - \Delta_{\mathrm{L}}^2})\left[f_{\mathrm{L}}(\varepsilon) - f_{\mathrm{R}}(\varepsilon)\right]\frac{\Delta_{\mathrm{L}}\Delta_{\mathrm{R}}}{\sqrt{\varepsilon^2 - \Delta_{\mathrm{L}}^2}}kdk$$

3. Thermal Josephson effect in graphene bilayers:

Transport

$$I_Q \approx \frac{16\pi|\Gamma|^2 k_B^2 T_R(T_L - T_R)}{3(\hbar v_F r)^2} \quad \text{(for } \varphi = 0\text{)}$$

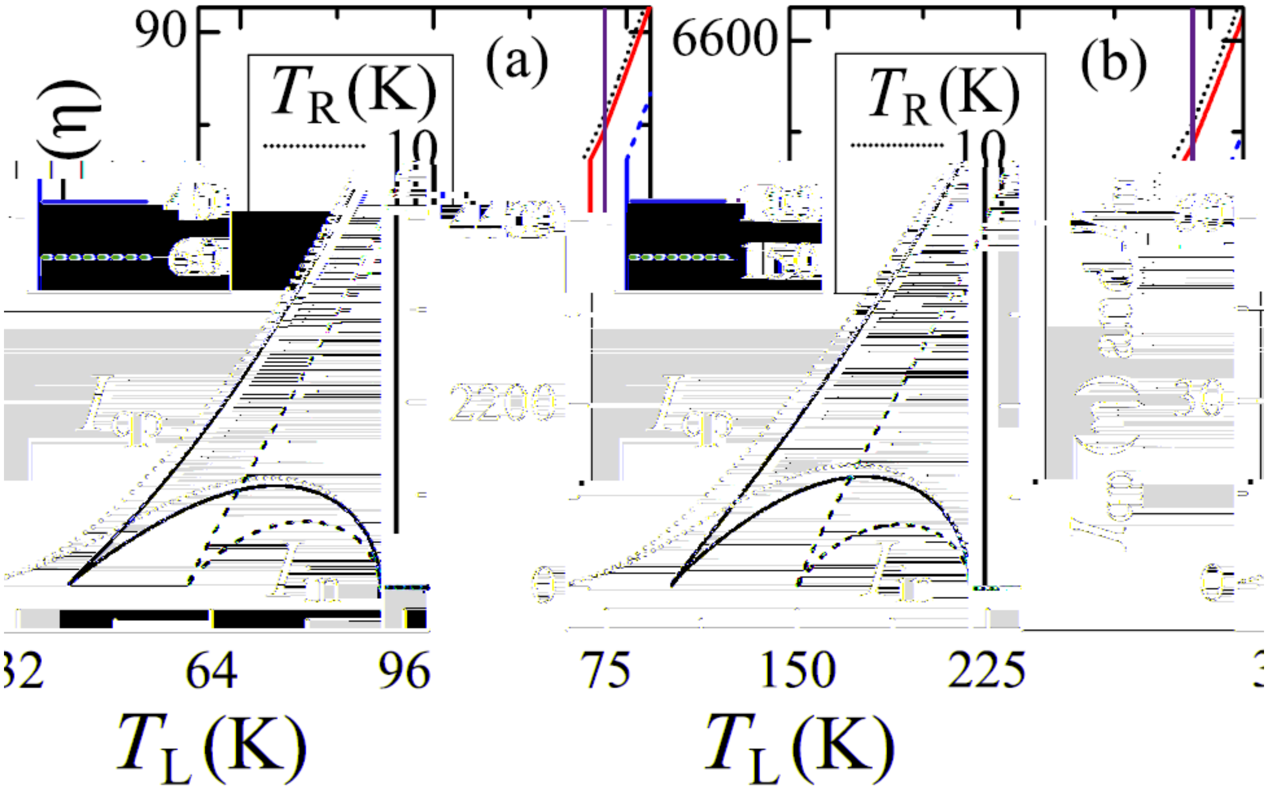

I_{qp} I_{in} T_L (a) (b)

r 20 nm 5 nm

3. Thermal Josephson effect in graphene bilayers:

Thermal rectification

$$\kappa = \frac{I_{LR} - I_{RL}}{I_{RL}}$$

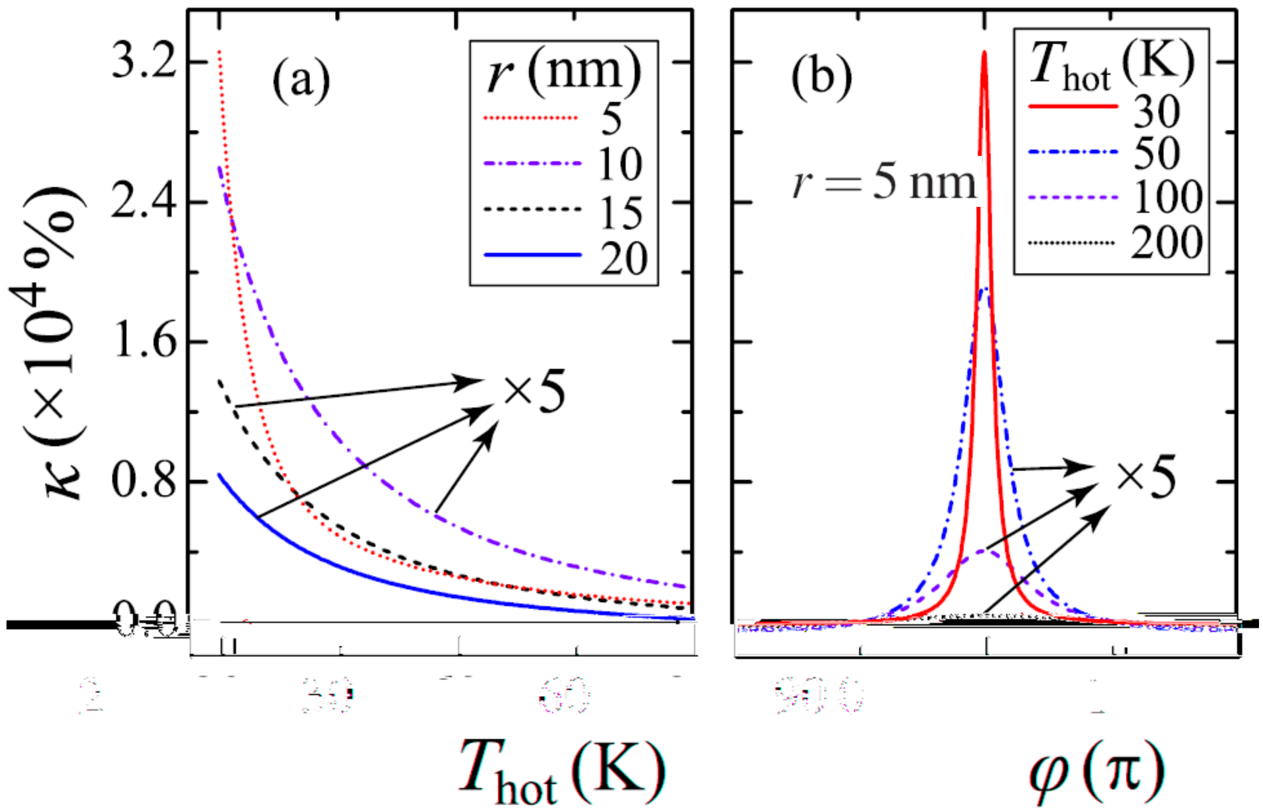

π

3.3 10^4

κ T_{hot}（b） 低 （ ） T_{cold}=20 K

3. Thermal Josephson effect in graphene bilayers:

Thermal logic gate

$$T_L = (80 - 70\cos\alpha)\ \mathrm{K}$$

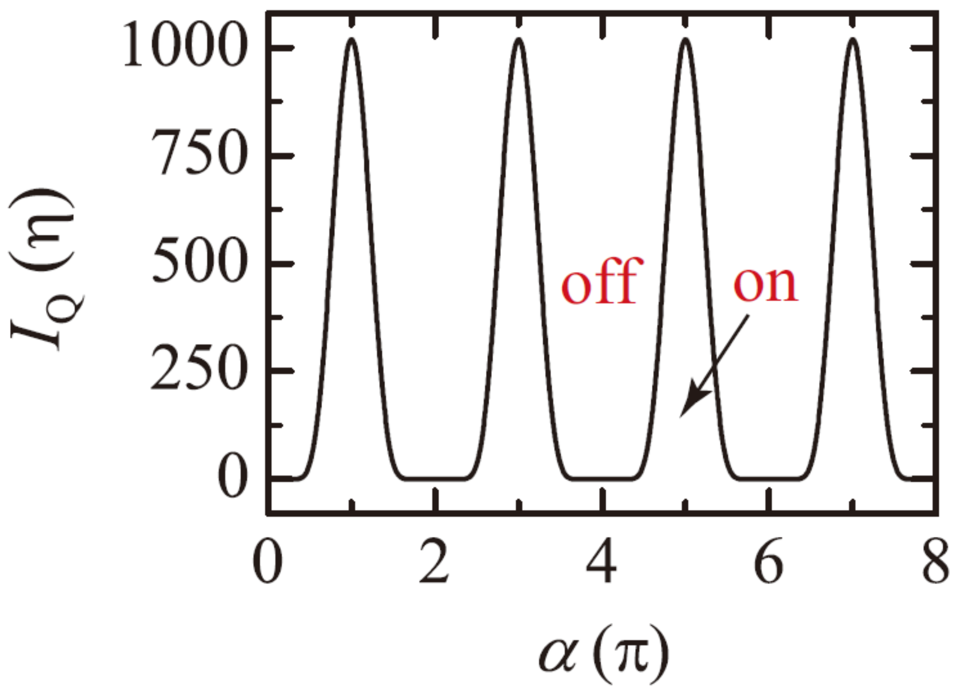

on

off

I_Q . T_R=10 K r = 5 nm

4. Summary: Some conclusions

For the exciton condensation in graphene bilayer and thermal Josephson effect in two coupled graphene bilayers, interesting results are

1) derived the criterion of criticality for exciton condensation;

2) obtained the phase diagram to distinguish BEC and BCS states;

3) investigated the thermal transport through a Josephson junction;

4) proposed physically two thermally controllable devices

X. Zhai and G. Jin, APL **102**, 023104 (2013).

X. Zhai and G. Jin, Spin **03**, 1330006 (2013).

X. Zhai and G. Jin, JPCM **26**, 015304 (2014).

1. Background: Graphene mono- and multi-layers

C. L. Kane and E. J. Mele, PRL 95, 226801, 146802 (2005).

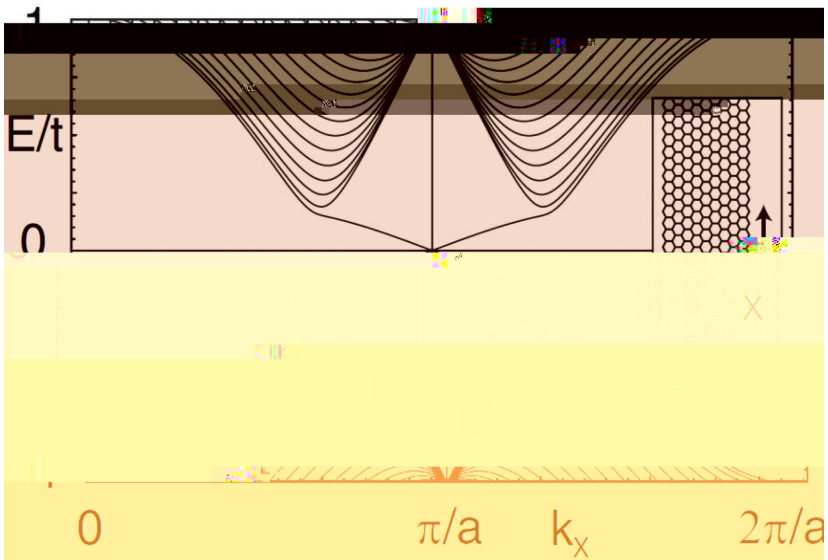

topologically nontrivial

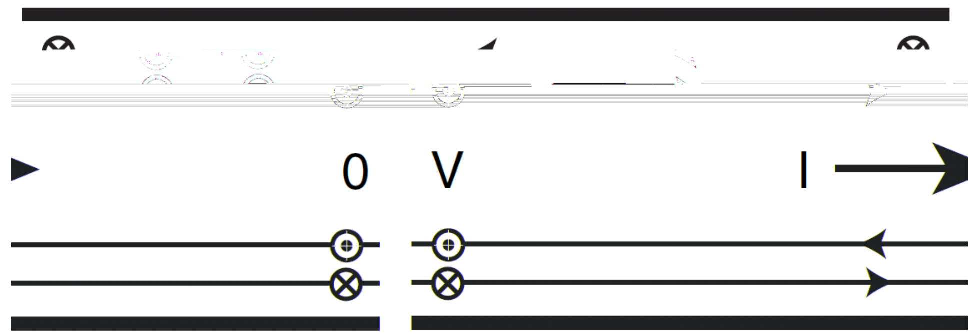

not a practical toplogical insulator (TI) because of weak intrinsic SO coupling

To engineer the TI phase in graphene
Theoretical studies have shown that graphene
phase under large Rashba interaction and a bias used to open a band-gap

C. Weeks *et al.*, PRX 1, 021001 (2011).

H. Jiang *et al*, PRL 109, 116803 (2012).

Z. Qiao *et al.*, PRL 107, 256801 (2011).

X. Li et al., PRB 85, 201404(R) (2012).

1. Background: HgTe/CdTe quantum wells

The first confirmation of TI theoretically and experimentally

B. A. Bernevig, T. L. Hughes, and S.-C. Zhang, Science 314, 1757 (2006);

M. Konig *et al.*, Science 318, 766 (2007).

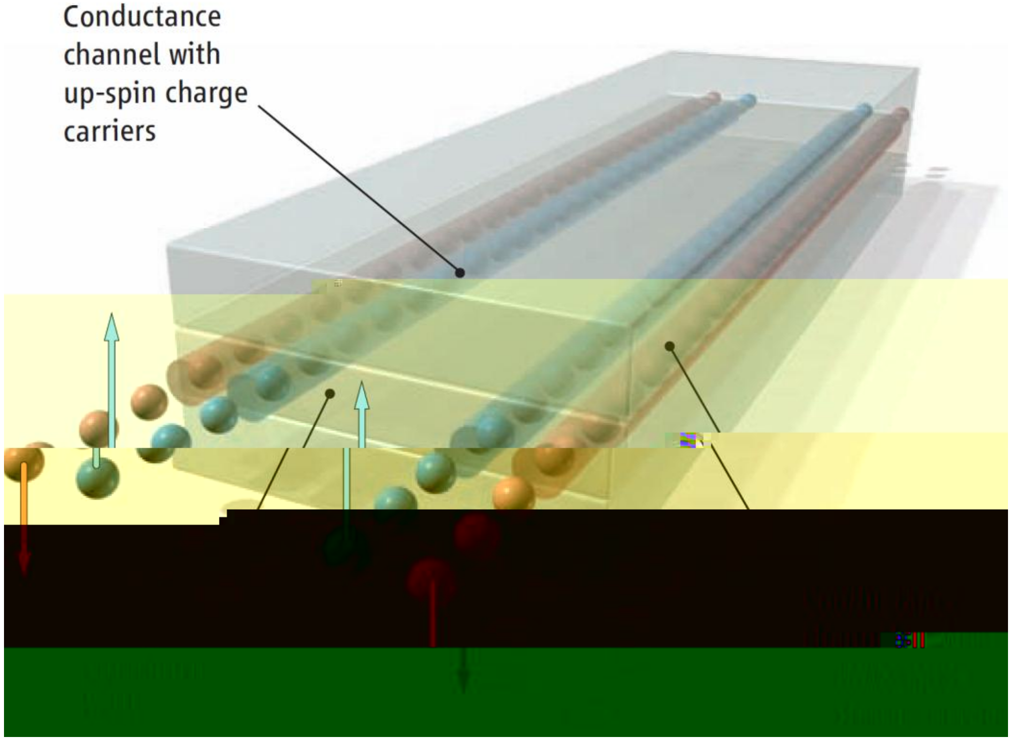

A variant material CdTe/Hg CdTe/CdTe quantum well is possible for transition between a normal insulator (NI) and a topological insulator by an electric field

J. Li and K. Chang, APL 95, 222110 (2009).

further expectation to explore the topological phase transition

1. Background: Boron-nitride mono- and multi-layers

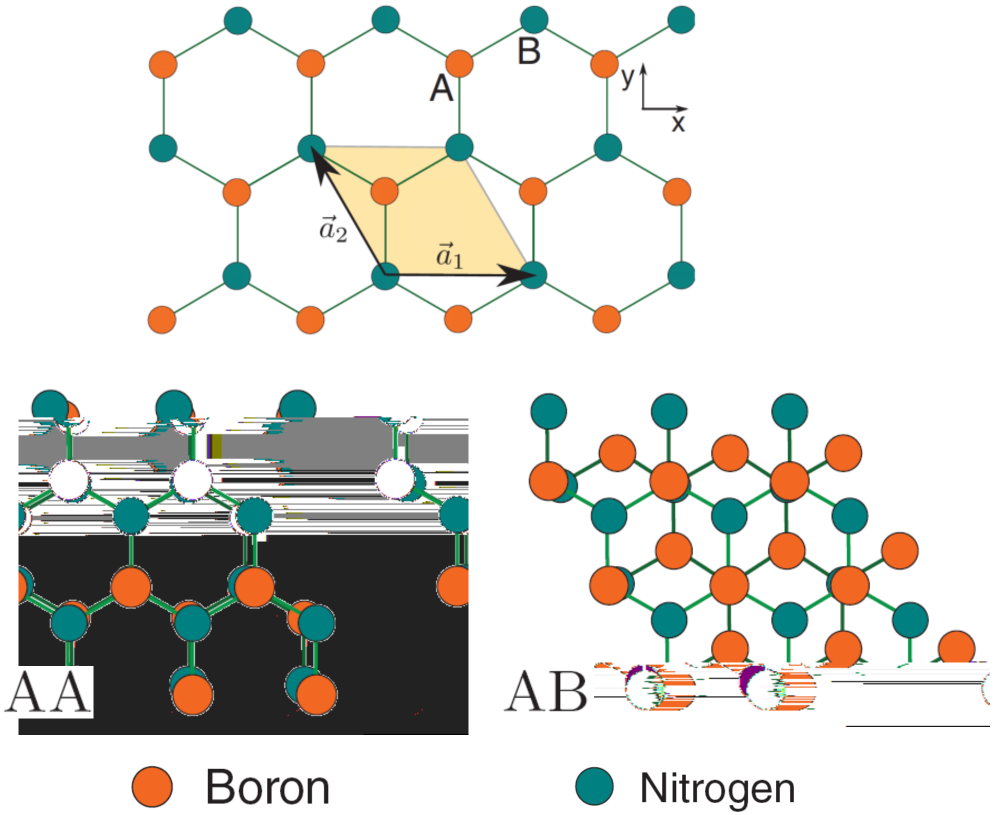

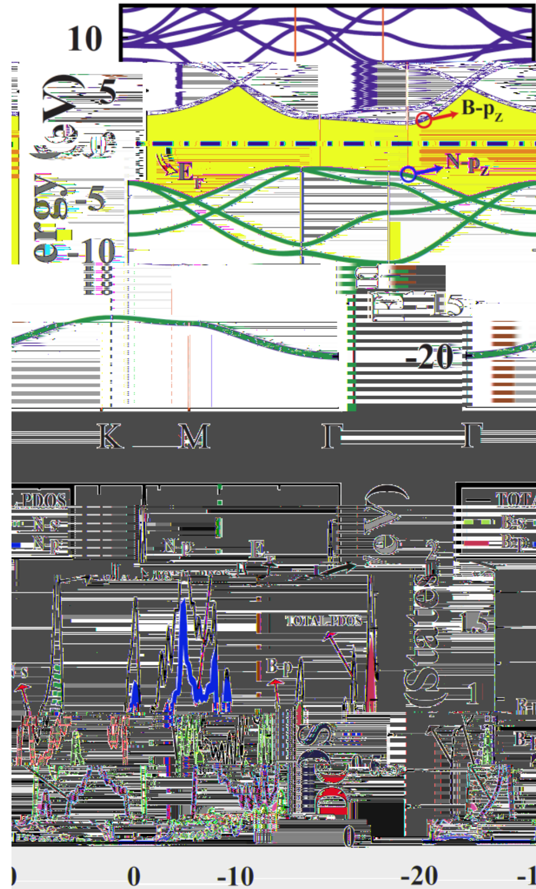

R. M. Ribeiro and N. M. R. Peres, PRB 83, 235312 (2011).

M. Topsakal, E. Aktürk, and S. Ciraci, PRB 79, 115442 (2009).

a hexagonal boron nitride (BN) layer is made out of strong polar covalent bonds and has no reflection symmetry. This leads to large band-gaps, about 4.6 eV for monolayer and 6 eV for single crystal

2. Object and Formulation: Boron-nitride bilayers

We ask Is it possible to realize the TI phase in large-gap BN materials?

We propose a way to significantly reduce their gaps to find TI phase!

Consider two stable stacked boron-nitride bilayers as in figures

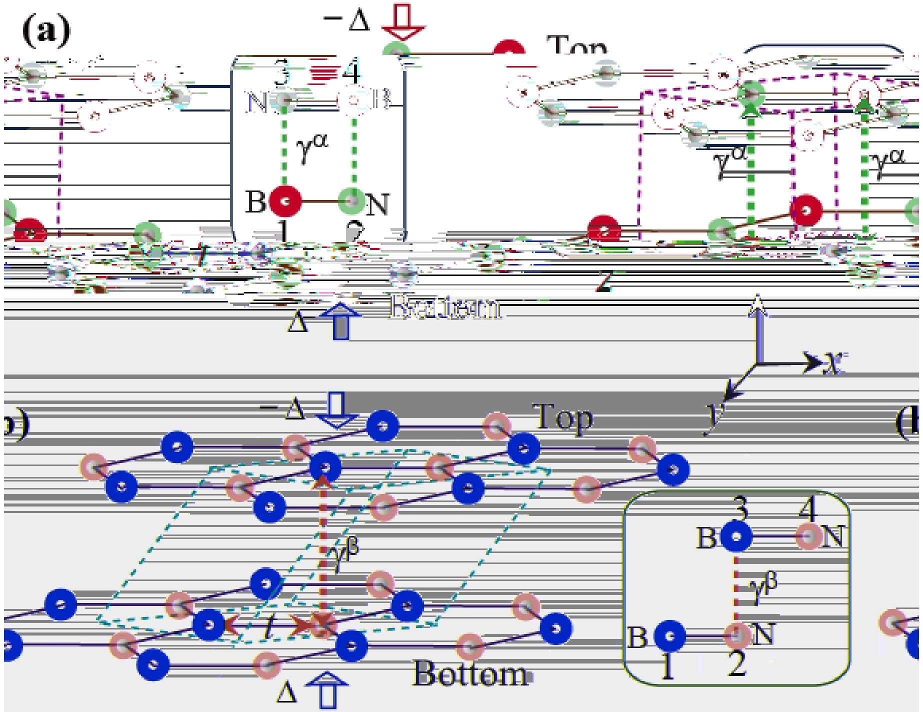

AA-stacked BNBL (α-BNBL)

potential energies created by a gate voltage

AB-stacked BNBL (β-BNBL)

Contrary to a graphene bilayer, the interlayer bias here is used to reduce the charge polarity of two trigonal sublattices in different layers and then to decrease the band-gaps of the two stackings

2. Object and Formulation: Model Hamiltonian

In the tight-binding approximation, Kane-Mele model + +

$$\mathcal{H} = \mathcal{H}_B + \mathcal{H}_T + \mathcal{H}_{BT} + \mathcal{H}_{TB}$$

$$\mathcal{H}_{B(T)} = \sum_{i\sigma}(\varepsilon_i \pm \Delta)c^\dagger_{i\sigma}c_{i\sigma} - t\sum_{\langle ij\rangle\sigma} c^\dagger_{i\sigma}c_{j\sigma} + i\lambda_{\mathrm{SO}}\sum_{\langle\langle ij\rangle\rangle\sigma\bar{\sigma}} \nu_{ij}\mathbf{S}_{\sigma\bar{\sigma}}\cdot z c^\dagger_{i\sigma}c_{j\bar{\sigma}} + i\lambda_R \sum_{\langle ij\rangle\sigma\sigma'} \left(\mathbf{S}_{\sigma\sigma'}\times \mathbf{d}_{ij}\right)\cdot z c^\dagger_{i\sigma}c_{j\sigma'}$$

$$\mathcal{H}_{BT}\ \gamma\ \gamma^{\alpha}\sum_{i\in B, j\in T,\sigma} c^\dagger_{i\sigma}c_{j\sigma}; \qquad \mathcal{H}_{TB}\ \gamma\ \gamma^{\beta}\sum_{i\in B, j\in T,\sigma} c^\dagger_{j\sigma}c_{i\sigma}$$

The energy spectra and physical properties $\longleftarrow$

$$G_{i\sigma,j\sigma'}(E) = \frac{1}{\Omega_{\mathrm{BZ}}}\int d\mathbf{k}\,\frac{e^{i\mathbf{k}\cdot(\mathbf{r}_{i\sigma}-\mathbf{r}_{j\sigma'})}}{E + i\eta - \mathcal{H}(\mathbf{k})}$$

$$\rho(E)\ g_\sigma(E) = -\frac{1}{\pi}\sum_{i=1}^{4}\mathrm{Im}\,G_{i\sigma,i\sigma}$$

2. Object and Formulation: Matrix representation

Hamiltonian in the momentum space, an 8×8 matrix

$$\mathcal{H}(\boldsymbol{k}) = \begin{pmatrix} \mathcal{H}_B(\boldsymbol{k}) & \mathcal{H}_{BT} \\ \mathcal{H}_{TB} & \mathcal{H}_T(\boldsymbol{k}) \end{pmatrix}$$

$$\mathcal{H}_{BT}^{\alpha} = \begin{pmatrix} \gamma^{\alpha}\mathbf{I} & 0 \\ 0 & \gamma^{\alpha}\mathbf{I} \end{pmatrix}, \quad \mathcal{H}_{BT}^{\beta} = \begin{pmatrix} 0 & 0 \\ \gamma^{\beta}\mathbf{I} & 0 \end{pmatrix}$$

$$\mathcal{H}_{B(T)}(\boldsymbol{k}) = \begin{pmatrix} \epsilon_{s1} + d(\boldsymbol{k}) & 0 & f(\boldsymbol{k}) & g_1(\boldsymbol{k}) \\ 0 & \epsilon_{s1} - d(\boldsymbol{k}) & g_2(\boldsymbol{k}) & f(\boldsymbol{k}) \\ f^*(\boldsymbol{k}) & g_2^*(\boldsymbol{k}) & \epsilon_{s2} - d(\boldsymbol{k}) & 0 \\ g_1^*(\boldsymbol{k}) & f^*(\boldsymbol{k}) & 0 & \epsilon_{s2} + d(\boldsymbol{k}) \end{pmatrix}$$

All the matrix elements are determined

$$d(\boldsymbol{k}) = 2\lambda_{\mathrm{SO}}\left[2\sin\left(\sqrt{3}k_y a/2\right)\cos(3k_x a/2) - \sin\left(\sqrt{3}k_y a\right)\right]$$

$$f(\boldsymbol{k}) = -t\mathrm{e}^{ik_x a}\left[1 + 2\mathrm{e}^{-i(3k_x a/2)}\cos\left(\sqrt{3}k_y a/2\right)\right]$$

$$g_1(\boldsymbol{k}) = -\lambda_{\mathrm{R}}\mathrm{e}^{ik_x a}\left[1 - 2\mathrm{e}^{-i(3k_x a/2)}\cos\left(\sqrt{3}k_y a/2 + \pi/3\right)\right]$$

$$g_2(\boldsymbol{k}) = \lambda_{\mathrm{R}}\mathrm{e}^{ik_x a}\left[1 - 2\mathrm{e}^{-i(3k_x a/2)}\cos\left(\sqrt{3}k_y a/2 - \pi/3\right)\right]$$

3. Main Results: (i) Bulk electronic structures

Dispersion relations and the densities of states (DOS) of (a) α-BNBL and (b) β-BNBL

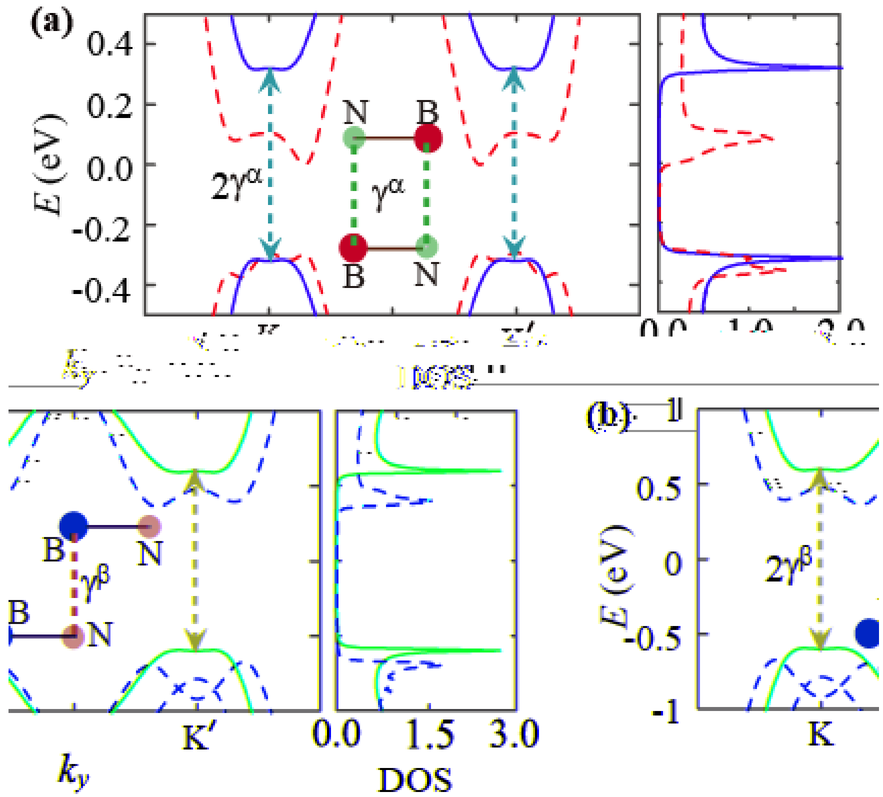

The influence of the SO couplings

Solid lines   Dashed lines

$\lambda_{SO} = \lambda_R = 0$ $\lambda_{SO} = 0.05t^{\alpha(\beta)}, \ \lambda_R = 0.2t^{\alpha(\beta)}$

The band-gaps are greatly reduced by the gate voltage, due to the decrease of the charge polarity. For $\Delta = \varepsilon_0^{\alpha(\beta)}$

$E_g^\alpha \cong 2\gamma^\alpha = 0.64\,\text{eV}$ $E_g^\beta \cong 2\gamma^\beta = 1.2\,\text{eV}$

$\ll$ 4.6 eV in natural BN layers

$$E^\alpha = \pm\sqrt{\Delta^2 + \left(\varepsilon_0^\alpha\right)^2 + (\gamma^\alpha)^2 + |f(\boldsymbol{k})|^2 \pm 2\sqrt{h^\alpha(\boldsymbol{k})}},$$

$$h^\alpha(\boldsymbol{k}) = \left|\gamma^\alpha f(\boldsymbol{k})\right|^2 + \Delta^2\left[\left(\varepsilon_0^\alpha\right)^2 + |f(\boldsymbol{k})|^2\right]$$

$$E^\beta = \pm\sqrt{\Delta^2 + \left(\varepsilon_0^\beta\right)^2 + \frac{1}{2}(\gamma^\beta)^2 + |f(\boldsymbol{k})|^2 \pm \sqrt{h^\beta(\boldsymbol{k})}}$$

$$h^\beta(\boldsymbol{k}) = 4\Delta^2\left[\left(\varepsilon_0^\beta\right)^2 + |f(\boldsymbol{k})|^2\right] - 2\Delta\varepsilon_0^\beta\left(\gamma^\beta\right)^2 + |\gamma^\beta f(\boldsymbol{k})|^2 + \frac{1}{4}\left(\gamma^\beta\right)^4$$

3. Main Results: (ii) Edge states and Z_2 topological index

Particular concern is to find the topological edge states for the confined boron-nitride bilayer nanoribbons (NR) in Figure

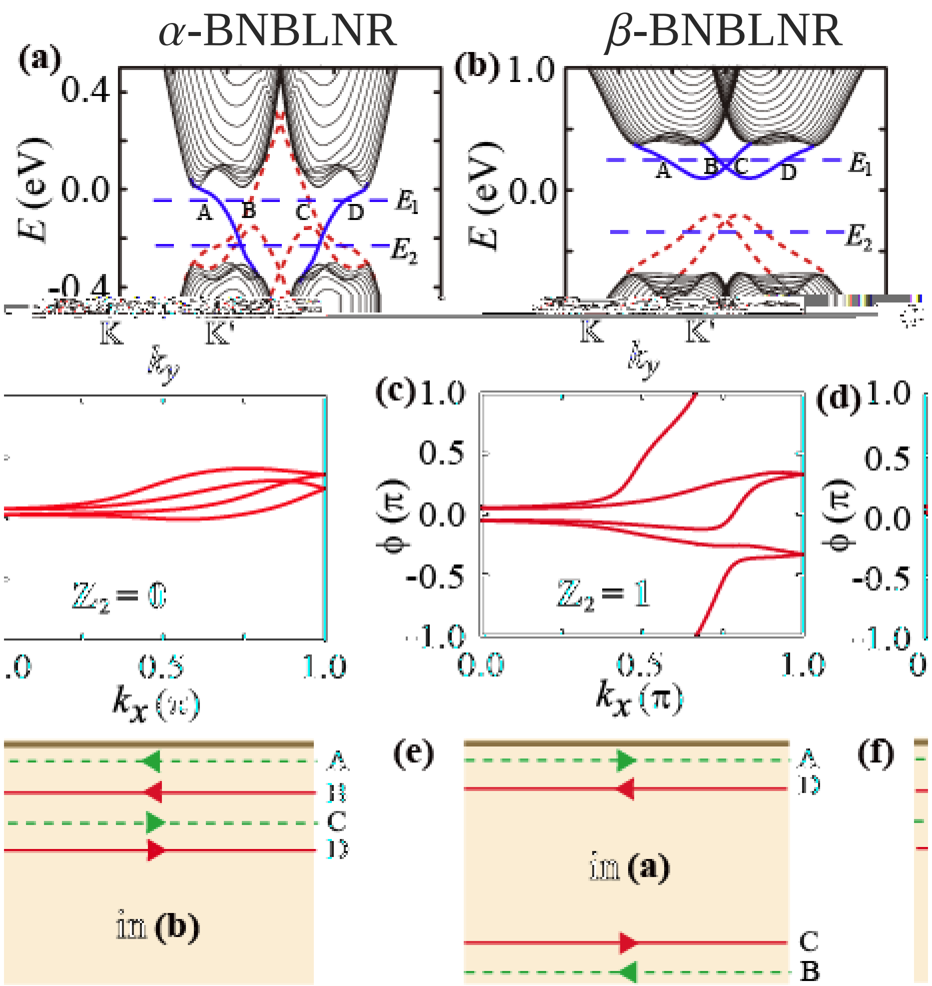

(a), (b) show the band structures of the α- and β-BNBLNRs with

$$\lambda_{\rm SO} = 0.05t^{\alpha(\beta)},\ \lambda_{\rm R} = 0.2t^{\alpha(\beta)}$$

There are edge states within the bulk gaps, their dispersion curves

(c), (d) illustrate the evolution lines of the Wannier function centers used

$$\Rightarrow \quad Z_2 = \sum_{n=1}^{4} T_n \bmod 2 = \begin{cases} 1, & \text{T I} \\ 0, & \text{not T I} \end{cases}$$

(e), (f) distribute the four edge states A, B, C, D in (a), (b). α-BNBLNR has the feature of TI, β-BNBLNR has not

3. Main Results: (iii) Phase diagram and edge transport

The condition of forming the topological edge states in the α-BNBLNR. For a nonzero ${}_{SO}$, obtain analytically

Two phase boudaries: $\lambda_R \sim \Delta$

$$\lambda = \frac{\sqrt{2}}{3}\sqrt{54\lambda_{SO}^2 - 9\lambda_{SO}\zeta \cdots}$$

$$\zeta = 12\lambda_{SO}(9\lambda_{SO} - \sqrt{3\eta_1})\eta_0$$

[redacted]

$$\gamma = \Delta - \varepsilon_0^{\alpha},\ \eta_1 = (\gamma^{\alpha})^2 + \gamma^2,\ \eta_2 = (\gamma^{\alpha})^2 + \Delta^2$$

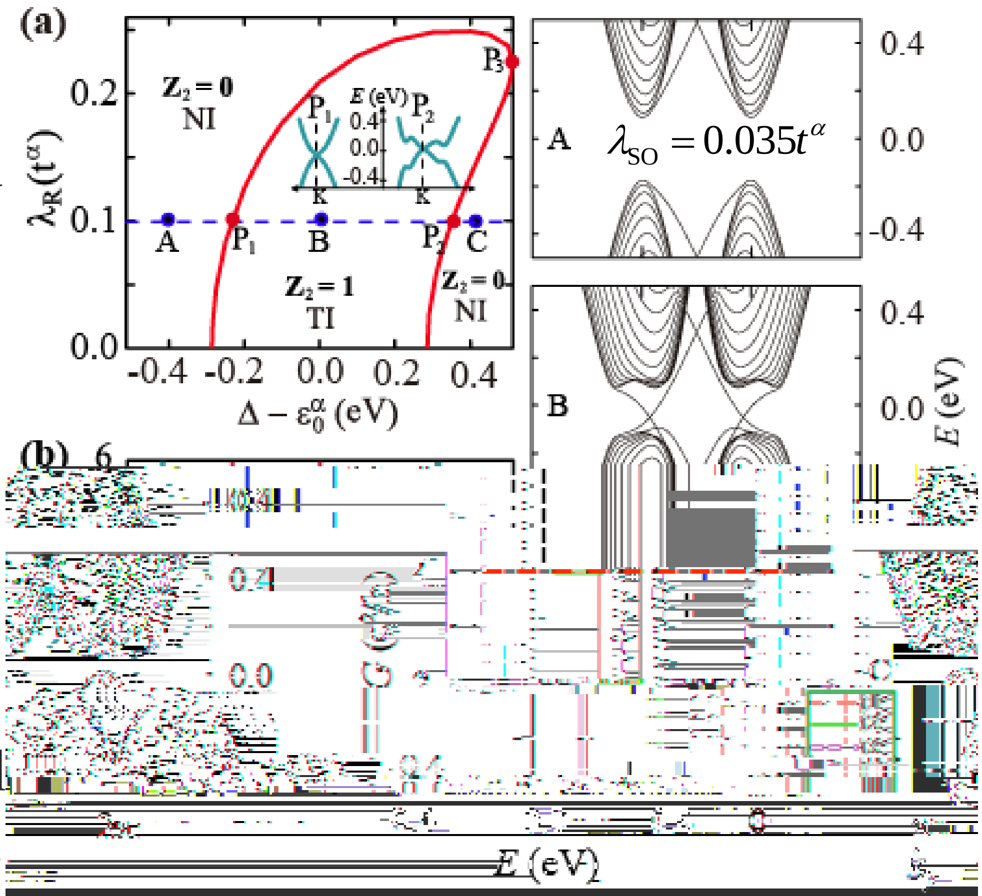

Figure (a) The phase diagram divided into three parts: NI, TI, NI; P_1, P_2, P_3; as the bias increases, the reentrant phase behavior takes place; right insets show the energy bands of three points A, B, C; for c

Figure (b) shows the quantized edge conductance ~ energy in the different constructions and parameters.

$$G(E) = e^2/h\,\mathrm{Tr}[\mathcal{G}^r(E)\Gamma_L(E)\mathcal{G}^a(E)\Gamma_R(E)]$$

4. Summary: Some conclusions

For large-gap boron nitride, bias voltage can drive it to

1) A strong TI phase has been found in the AA-stacked BNBL, while the AB-stacked BNBL is impossible to become a TI.
2) For the AA-stacked BNBL, a reentrant behavior from an NI phase to a TI phase and then to an NI phase has been confirmed, and the two phase boundaries have been analytically given.
3) For the AB-stacked BNBL, four degenerate low-energy edge states are localized at a single edge

X. Zhai and G. Jin, PRB **89**, 085430 (2014).

1. Background: Chirality and Berry phase

GML:

$$\mathcal{H}_{\mathbf{K}} = v_F\,\boldsymbol{k}.\hat{\boldsymbol{\sigma}} = \hbar v_F \begin{pmatrix} 0 & k_x - ik_y \\ k_x + ik_y & 0 \end{pmatrix} \hbar$$

$$E(\boldsymbol{k}) = \pm \hbar v_F |\boldsymbol{k}|$$

$$\psi_{\pm,\mathbf{K}}(\boldsymbol{k}) = \frac{1}{\sqrt{2}} \begin{pmatrix} 1 \\ \pm e^{i\theta_{\boldsymbol{k}}} \end{pmatrix}$$

GBL:

$$\mathcal{H}_{\mathbf{K}} = -\frac{\hbar^2}{2m^*} \begin{pmatrix} 0 & (k_x - ik_y)^2 \\ (k_x + ik_y)^2 & 0 \end{pmatrix}$$

$$E(\boldsymbol{k}) = \pm \frac{(\hbar \boldsymbol{k})^2}{2m^*}$$

$$\psi_{\pm,\mathbf{K}}(\boldsymbol{k}) = \frac{1}{\sqrt{2}} \begin{pmatrix} 1 \\ \mp e^{2i\theta_{\boldsymbol{k}}} \end{pmatrix}$$

$$\hat{C} \equiv \frac{\boldsymbol{k} \cdot \hat{\boldsymbol{\sigma}}}{k}$$

$$\Phi_B = i \oint_C dk \left\langle \psi(k) \middle| \frac{\partial}{\partial k} \middle| \psi(k) \right\rangle$$

Berry phase-π

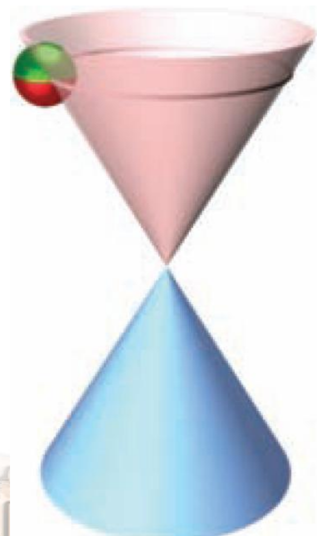

Berry phase-2π

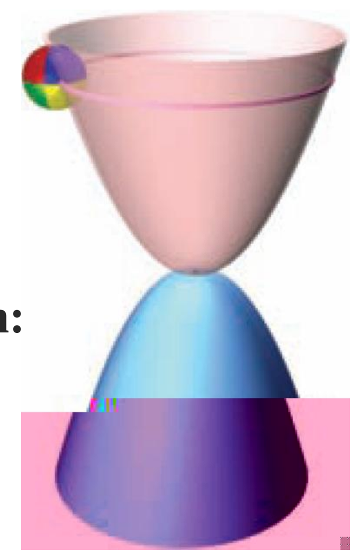

Berry phase in graphene from quantum Hall effect:

Y. Zhang et al., Nature 438, 201 (2005).

K. S. Novoselov et al., Nat. Phys. 2, 177 (2006).

Berry phase in graphene from weak antilocalization:

X. Wu et al., PRL 98, 136801 (2007).

Berry phase in graphene from photoemission:

Y. Liu et al., PRL 107, 166803 (2011).

1. Background: Andreev reflection

GML: C. W. J. Beenakker, PRL 97, 067007 (2006). ”Specular Andreev reflection in graphene

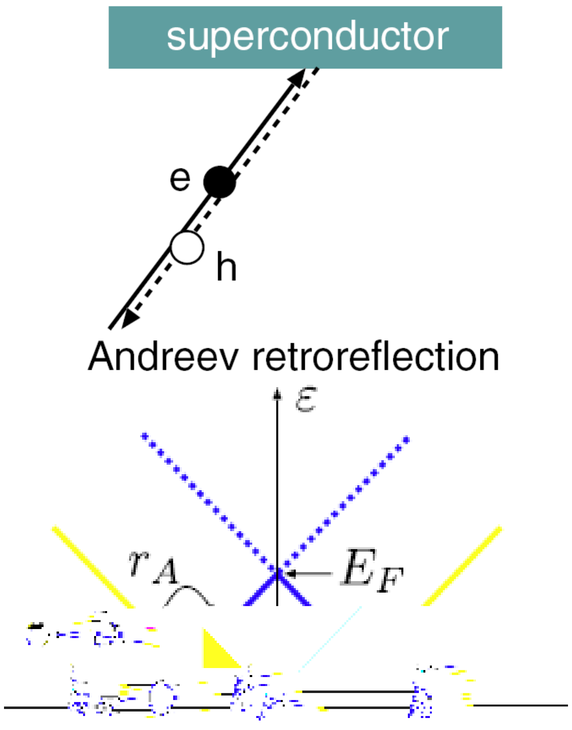

Andreev retroreflection

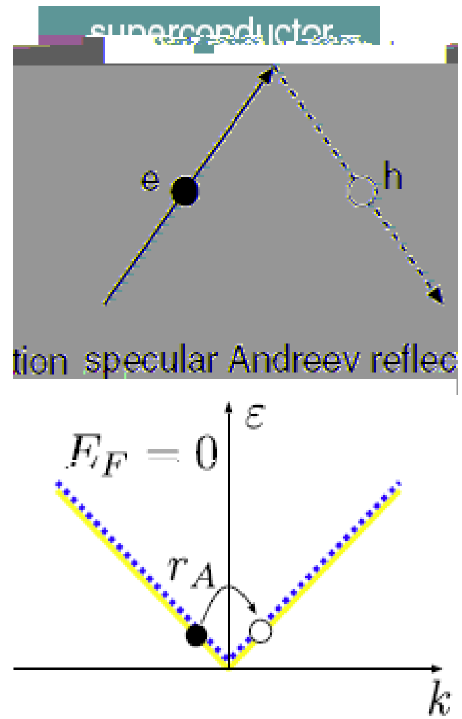

specular Andreev reflection

;

GBL: T. Ludwig, PRB 75, 195322 (2007). ”Andreev reflection in bilayer graphene

1. Background: Theoretical treatment

Bogoliubov-de Gennes (BdG) 方程

$$\begin{pmatrix} \mathcal{H}_{\mathrm{K(K')}} - E_{\mathrm{F}} & \Delta_0 e^{i\phi}\Theta(x) \\ \Delta_0 e^{-i\phi}\Theta(x) & E_{\mathrm{F}} - \mathcal{H}_{\mathrm{K(K')}} \end{pmatrix} \begin{pmatrix} u \\ v \end{pmatrix} = \varepsilon \begin{pmatrix} u \\ v \end{pmatrix}$$

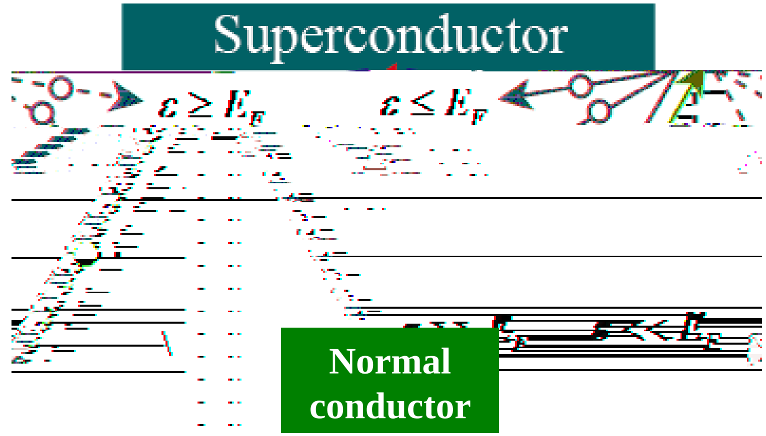

$$\varepsilon = |E_{\mathrm{F}} \pm \hbar v_{\mathrm{F}} \sqrt{k_x^2 + k_y^2}|$$

(both no Rashiba coupling)

GML:

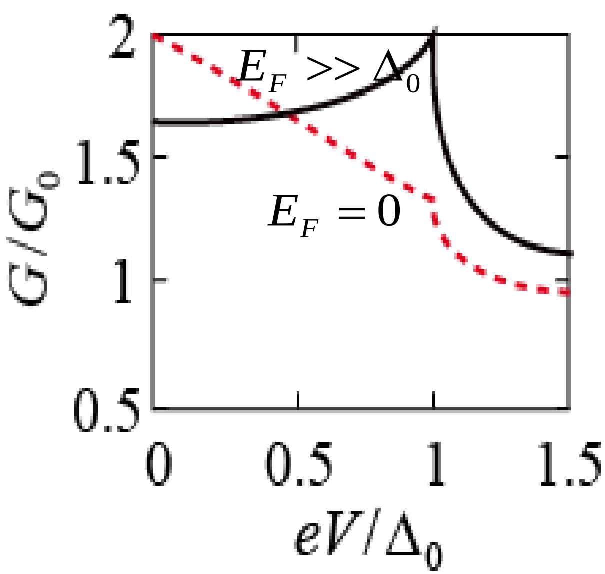

GBL:

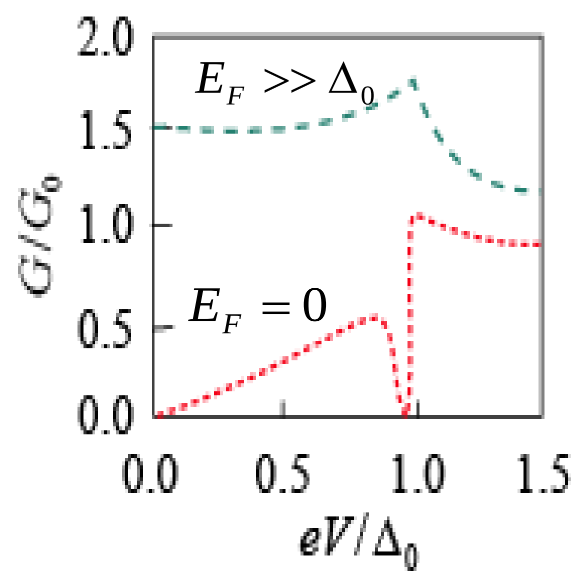

2. Object and Formulation: Rashba

；D. Marchenko et. al., Nature Commun. 3, 1232 (2012).

$$H = t\sum_{\langle ij\rangle} c_i^\dagger c_j + i\lambda_R \sum_{\langle ij\rangle} c_i^\dagger (\mathbf{s}\times\hat{\mathbf{d}}_{ij})_z c_j$$

$\lambda_R = 0$ $\lambda_R \neq 0$

带

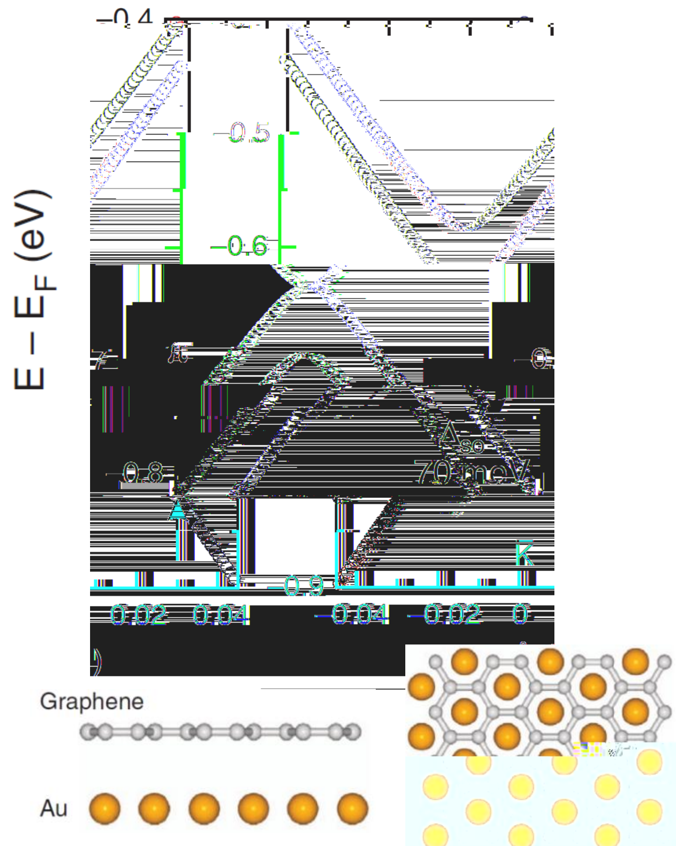

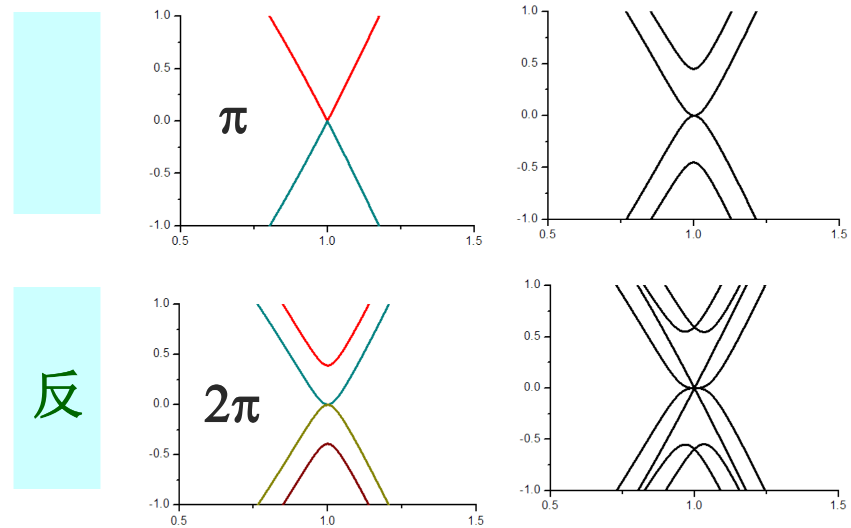

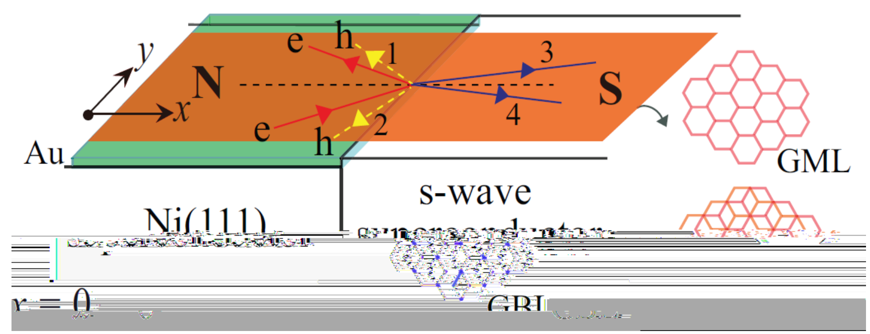

兴 Rashba E. I. Rashba, Phy. Rev. B, 79, 161409(R) (2009).

左 ； M.-H. Liu, et al., Phy. Rev. B, 85, 085406 (2012).

In ； Z. Jia et al., Phys. Rev. B 91, 085411 (2015).

2. Object and Formulation: 。 Berry 低

Matrix representation with Rashiba interaction

$$\mathcal{H}_\xi = \hbar v_F(\sigma_x k_x + \xi\sigma_y k_y)\otimes s_0 + \frac{\lambda_R}{2}(\sigma_x\otimes s_y - \xi\sigma_y\otimes s_x)$$

$$E_{\mu\nu}(k) = \frac{\mu\nu}{2}\left(\sqrt{\lambda_R^2 + 4(\hbar v_F k)^2} - \nu\lambda_R\right)$$

$$\psi^{K}_{\mu+} = c_0(i\mu\varrho e^{-i\theta}, \mu\varrho', i\varrho', \varrho e^{i\theta})^T$$

$$\psi^{K}_{\mu-} = c_0(i\mu\varrho' e^{-i\theta}, -\mu\varrho, -i\varrho, \varrho' e^{i\theta})^T$$

$$\psi^{K'}_{\mu+} = c_0(\mu\varrho', -i\mu\varrho e^{i\theta}, \varrho e^{-i\theta}, -i\varrho')^T$$

$$\psi^{K'}_{\mu-} = c_0(-\mu\varrho, -i\mu\varrho' e^{i\theta}, \varrho' e^{-i\theta}, i\varrho)^T$$

$\varrho = \cos(\vartheta/2)$， $\varrho' = \sin(\vartheta/2)$

$$\Phi_B = i\int_0^{2\pi} d\theta \left\langle \psi^\xi_{\mu\nu}\left|\frac{\partial}{\partial\theta}\right|\psi^\xi_{\mu\nu}\right\rangle = 0$$

可以证明，使用另外的一个规范，用 $\psi^\xi_{\mu\nu}$ 乘以$e^{-i\theta}$，[illegible]变成 2π。因此，规范只是改变了赝自旋的绕数

$\boxed{\text{Berry 相位从 } \pi\ (\lambda_R = 0) \text{ 变为 } 2\pi\ (\lambda_R \neq 0)}$

反

$$\mathcal{H}_\xi = H^0_\xi + H^R_\xi = -\frac{(\hbar v_F k)^2}{\gamma}\begin{pmatrix} 0 & e^{-2i\xi\theta} \\ e^{2i\xi\theta} & 0 \end{pmatrix}\otimes s_0$$

$$-\frac{\hbar v_F\lambda_R}{\gamma}[\sigma_x\otimes(k_x s_y + k_y s_x) - \xi\sigma_y\otimes(k_x s_x - k_y s_y)]$$

$$E_{\mu\nu}(k) = \frac{\mu\hbar v_F k}{\gamma}\left(\sqrt{\lambda_R^2 + (\hbar v_F k)^2} - \nu\lambda_R\right)$$

$$\psi^{K}_{\mu+} = c_0(-i\mu\varrho e^{-2i\theta}, -\mu\varrho' e^{-i\theta}, i\varrho', \varrho e^{i\theta})^T$$

$$\psi^{K}_{\mu-} = c_0(i\mu\varrho' e^{-2i\theta}, -\mu\varrho e^{-i\theta}, -i\varrho, \varrho' e^{i\theta})^T$$

$$\psi^{K'}_{\mu+} = c_0(-\mu\varrho' e^{i\theta}, i\mu\varrho e^{2i\theta}, \varrho e^{-i\theta}, -i\varrho')^T$$

$$\psi^{K'}_{\mu-} = c_0(-\mu\varrho e^{i\theta}, -i\mu\varrho' e^{2i\theta}, \varrho' e^{-i\theta}, i\varrho)^T$$

[illegible]

$$\Phi_B = i\int_0^{2\pi} d\theta \left\langle \psi^\xi_{\mu\nu}\left|\frac{\partial}{\partial\theta}\right|\psi^\xi_{\mu\nu}\right\rangle = \begin{cases} \pi, & \text{for } \psi^{K}_{\mu\nu} \\ -\pi, & \text{for } \psi^{K'}_{\mu\nu} \end{cases}$$

$\boxed{\text{Berry 相位从 } 2\pi\ (\text{对于 } \lambda_R = 0) \text{ 变为 } \pi\ (\text{对于 } \lambda_R \neq 0)}$

3. Main Results: Rashba Berry 低

E_F=0 K K′

反

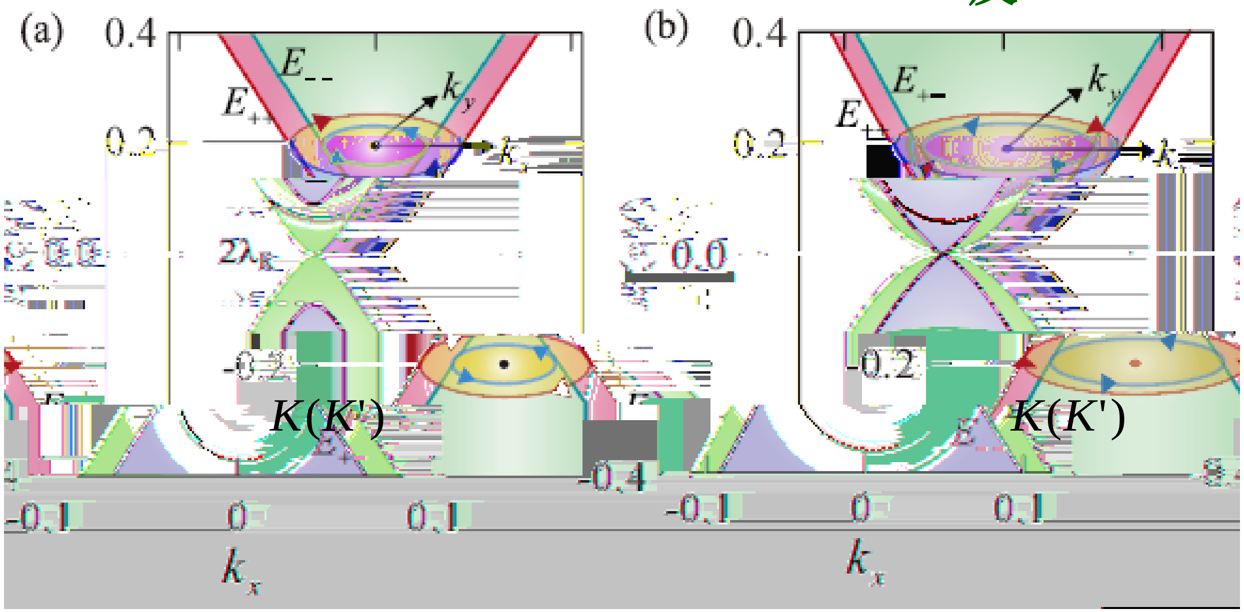

$$\langle \sigma_0 \otimes s \rangle_{\mu\nu} = (\boldsymbol{e}_k \times \boldsymbol{z})\, \nu \sin\vartheta \qquad \langle \sigma_0 \otimes s \rangle_{\mu\nu} = (\boldsymbol{e}_k \times \boldsymbol{z})\, \nu \sin\vartheta$$

$$\langle \sigma \otimes s_0 \rangle_{\mu\nu} = \boldsymbol{e}_k\, \mu\nu \sin\vartheta$$

$$+ \xi \boldsymbol{y} \sin(2\theta)]$$

下面考虑：NS 结上的电子-空穴转换！

3. Main Results: Analysing incidence and reflection

BdG equation

$$\begin{pmatrix} \mathcal{H}_\xi(x) - E_F & \Delta\Theta(x) \\ \Delta^*\Theta(x) & E_F - \mathcal{H}_\xi(x) \end{pmatrix}\begin{pmatrix} u \\ v \end{pmatrix} = \varepsilon\begin{pmatrix} u \\ v \end{pmatrix}$$

Excitation spectrum

$$\varepsilon_{\mu\nu} = \frac{1}{2}\left|\sqrt{\lambda_R^2 + 4(\hbar v_F k)^2} - \nu\lambda_R - 2\mu\nu E_F\right| \quad \text{(N)}$$

$$\varepsilon_{\mu\nu} = \sqrt{\Delta_0^2 + (E_F' + \mu\nu\cdot\hbar v_F k)^2} \quad \text{(S)}$$

Taking an example: Equal energy surface of GML

I: $E_F = 0 \ll \Delta_0$

II: $E_F \gg \Delta_0$

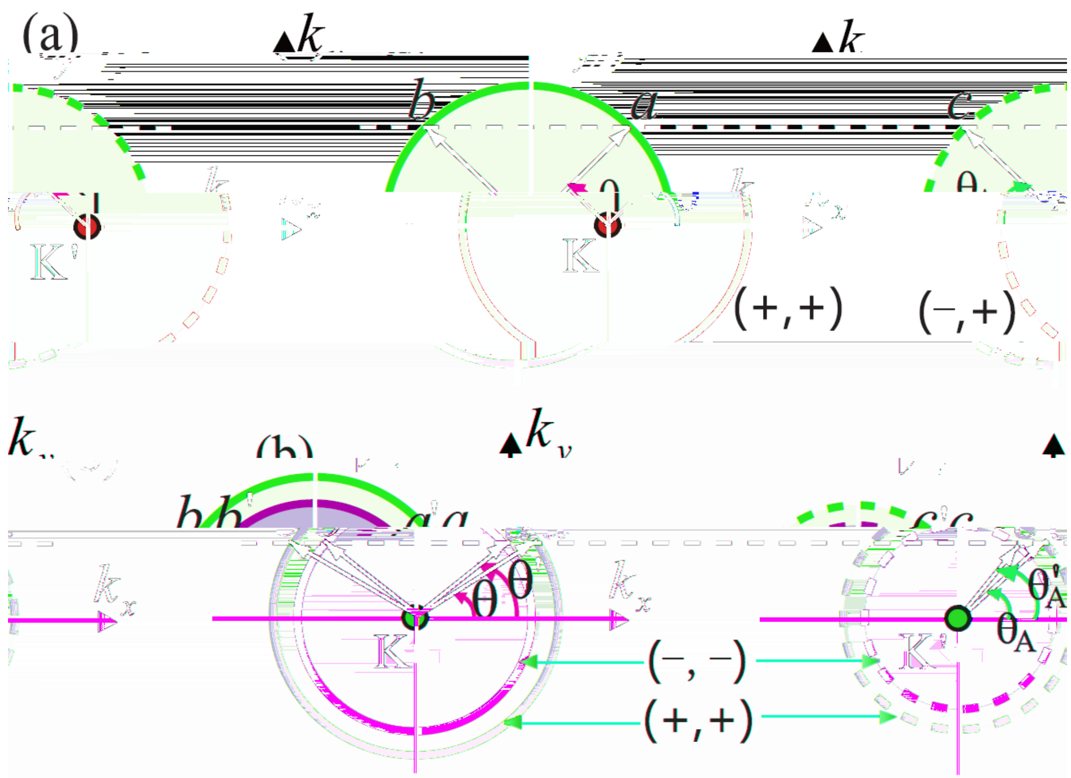

3. Main Results: Excitation spectra at normal incidence

I: $E_F=0$ **II:** $E_F \gg \Delta_0$

GML

GBL

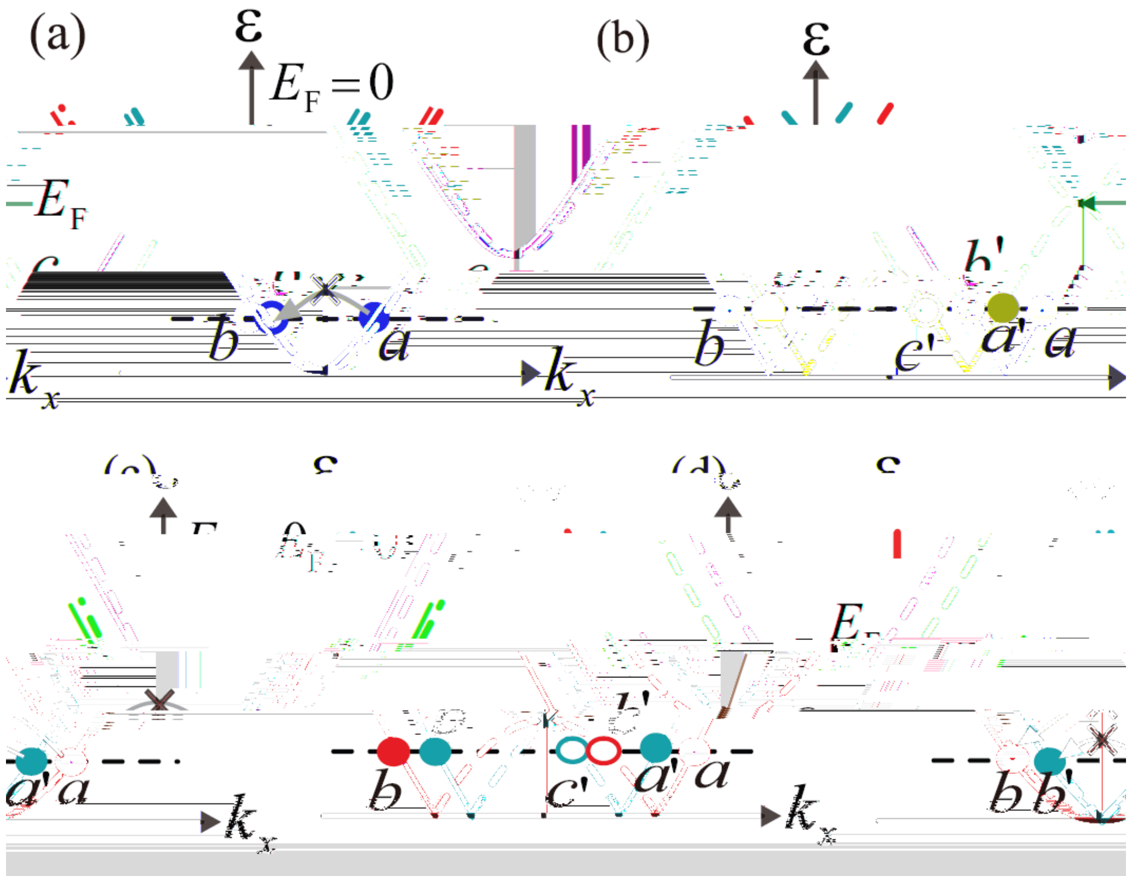

$$\varepsilon_{\nu\mu} = \sqrt{\Delta_0^2 + [E'_F + \mu(\hbar v_F k)^2/\gamma]^2}$$

3. Main Results: Interface scattering at an NS junction

The problem can be studied by using the BTK formalism, i.e., solving the BdG equations in both sides of the junction subject to the boundary conditions at the interface

BTK formula: multiband scattering

$$|a\rangle + (r_1|b\rangle + r_2|b'\rangle) + (r_{A_1}|c\rangle + r_{A_2}|c'\rangle) = (t_{1+}|f_+\rangle + t_{2+}|g_+\rangle) + (t_{1-}|f_-\rangle + t_{2-}|g_-\rangle),$$

$$\frac{G}{G_0} = \frac{1}{\mathcal{N}_0}\int_0^{\pi/2} d\theta \cos\theta \Big[\mathcal{N}_1\Big(1 - |r_1|^2 - P_{b'}|r_2|^2 + P_c|r_{A_1}|^2 + P_{c'}|r_{A_2}|^2\Big) + \mathcal{N}_2\Big(1 - |r_1'|^2 - P_{b'}|r_2'|^2 + P_c|r_{A_1}'|^2 + P_{c'}|r_{A_2}'|^2\Big)\Big]$$

$$G_0 \equiv \partial I_0/\partial V = (2e^2/h)\mathcal{N}_0$$

G. E. Blonder, M. Tinkham, and T. M. Klapwijk, PRB 25, 4515 (1982).

3. Main Results:

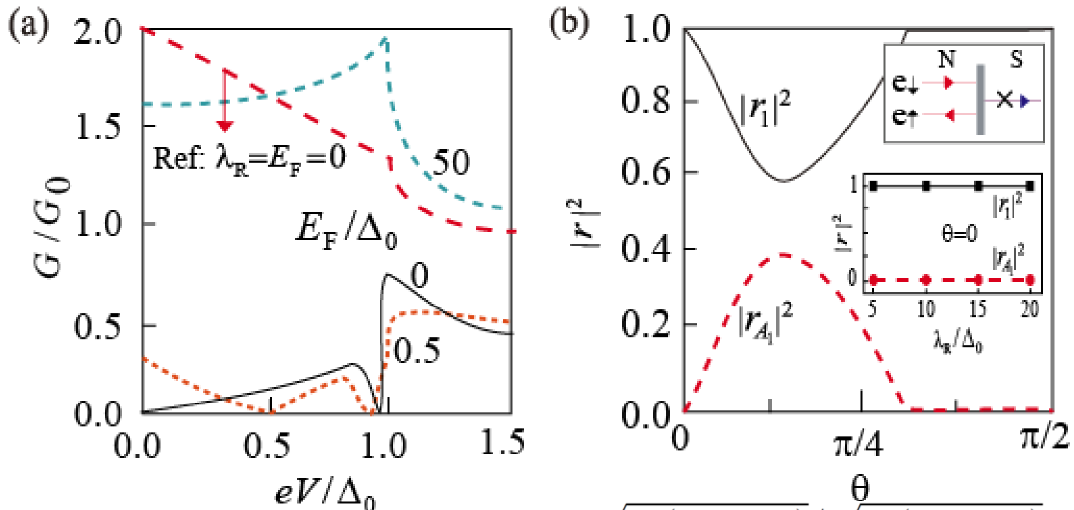

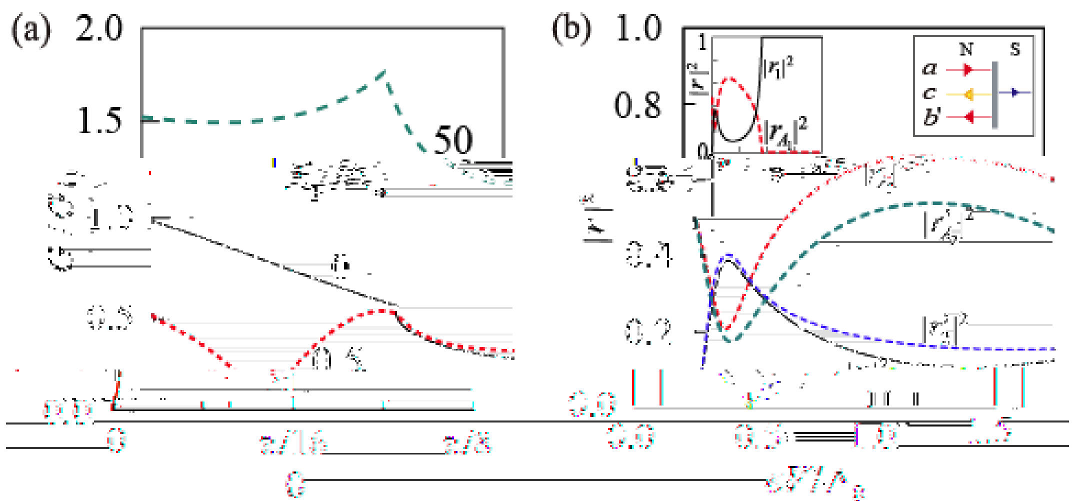

反

; **Blonder-Tinkham-Klapwijk**

4. Summary: Some conclusions

Rashba 反

1. Rashba 。 反 Berry 低

; π 2π, 反 2π π

2. Berry 低 – –

Andreev

3. Berry –

4.

X. Zhai and G. Jin, PRB **89**, 235416 (2014).

X. Zhou, Y. Xu, and G. Jin, in preparation.

1. Background；

, , **38**,409 (2009).
gaphene

SiC 下 Berry

: meV 下 meV

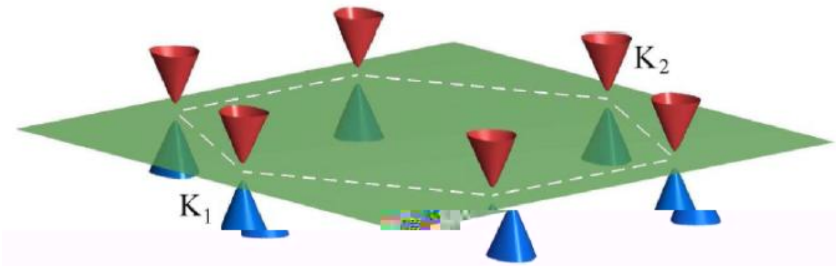

Berry

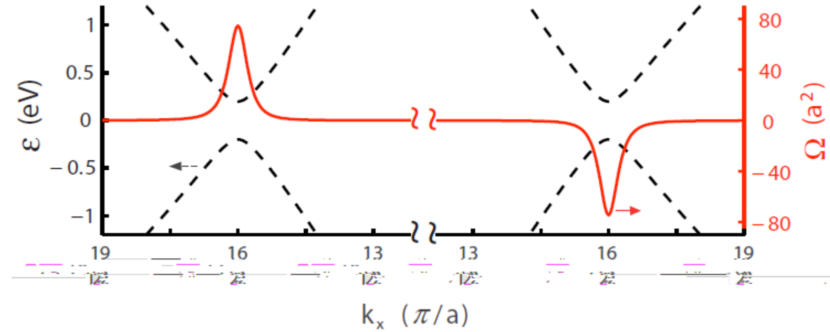

$$\mathcal{H}_{0,\xi}(\boldsymbol{k}) = \hbar v_F(\sigma_x k_x + \xi\sigma_y k_y)$$

$$\mathcal{H}_{s,\xi}(\boldsymbol{k}) = \mathcal{H}_{0,\xi}(\boldsymbol{k}) + \Delta\sigma_z$$

$$\boldsymbol{v}_n(\boldsymbol{k}) = \frac{\partial\varepsilon_n(\boldsymbol{k})}{\hbar\partial\boldsymbol{k}} - \frac{e}{\hbar}\boldsymbol{E}\times\boldsymbol{\Omega}_n(\boldsymbol{k})$$

$$\boldsymbol{\Omega}_n(\boldsymbol{k}) = i\langle\boldsymbol{\nabla}_k u_n(\boldsymbol{k})| \times |\boldsymbol{\nabla}_k u_n(\boldsymbol{k})\rangle$$

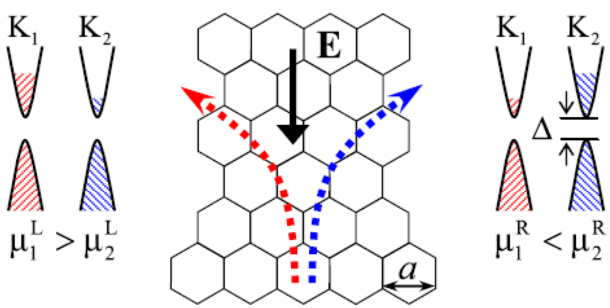

$$\Omega_-(\boldsymbol{k}) = -\xi\frac{(\hbar v_F)^2\Delta}{2[\Delta^2 + (\hbar v_F k)^2]^{3/2}}$$

Hall 底

D. Xiao, W. Yao, and Q. Niu, PRL **99**, 236809 (2007).

D. Xiao, M-C. Chang, and Q. Niu, RMP **82**, 1959 (2010).

$$= \frac{1}{T}\int_0^T$$

44.5 49.(2011).

2. Our Motivation:

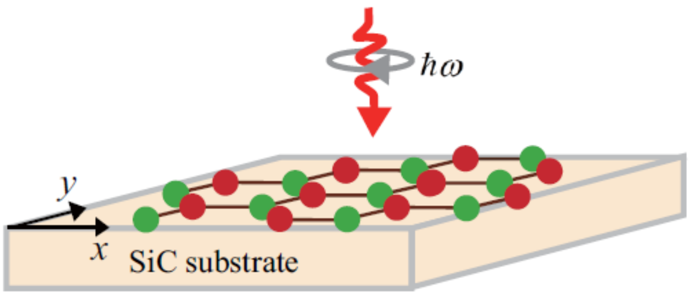

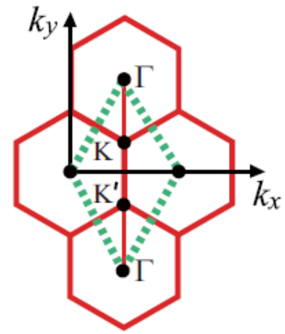

$$\boldsymbol{A}(t) = A_x(t)\boldsymbol{e}_x + A_y(t)\boldsymbol{e}_y = A[\eta\sin(\omega t)\boldsymbol{e}_x + \cos(\omega t)\boldsymbol{e}_y]$$

$$\mathcal{H}_\xi(\boldsymbol{k}, t) = \hbar v_{\mathrm{F}}\left[\sigma_x\left(k_x + \frac{eA_x(t)}{\hbar}\right) + \xi\sigma_y\left(k_y + \frac{eA_y(t)}{\hbar}\right)\right] + \Delta\sigma_z$$

$$\mathcal{H}_{\mathrm{F},\xi}(\boldsymbol{k}) \simeq \mathcal{H}_{0,\xi}(\boldsymbol{k}) + \frac{[\mathcal{H}_{-1,\xi}, \mathcal{H}_{+1,\xi}]}{\hbar\omega}$$

$$\mathcal{H}_{m,\xi}(\boldsymbol{k}) = \frac{1}{T}\int_0^T dt e^{im\omega t}\mathcal{H}_\xi(\boldsymbol{k}, t)$$

3. Results and Discussion：

$$\mathcal{H}_{\mathrm{F},\xi}(\boldsymbol{k}) = \mathcal{H}_{0,\xi}(\boldsymbol{k}) + \xi F_\eta(A)\sigma_z + \Delta\sigma_z$$

[redacted]

$$= \begin{pmatrix} \Delta + \xi F_\eta(A) & \hbar v_{\mathrm{F}}(k_x - i\xi k_y) \\ \hbar v_{\mathrm{F}}(k_x + i\xi k_y) & -\Delta - \xi F_\eta(A) \end{pmatrix}$$

$$E_\xi(\boldsymbol{k}) = \lambda\sqrt{(\Delta + \xi F_\eta)^2 + (\hbar v_{\mathrm{F}} k)^2} \qquad E_{\xi,\mathrm{g}} = 2|\Delta + \xi F_\eta(\omega)|$$

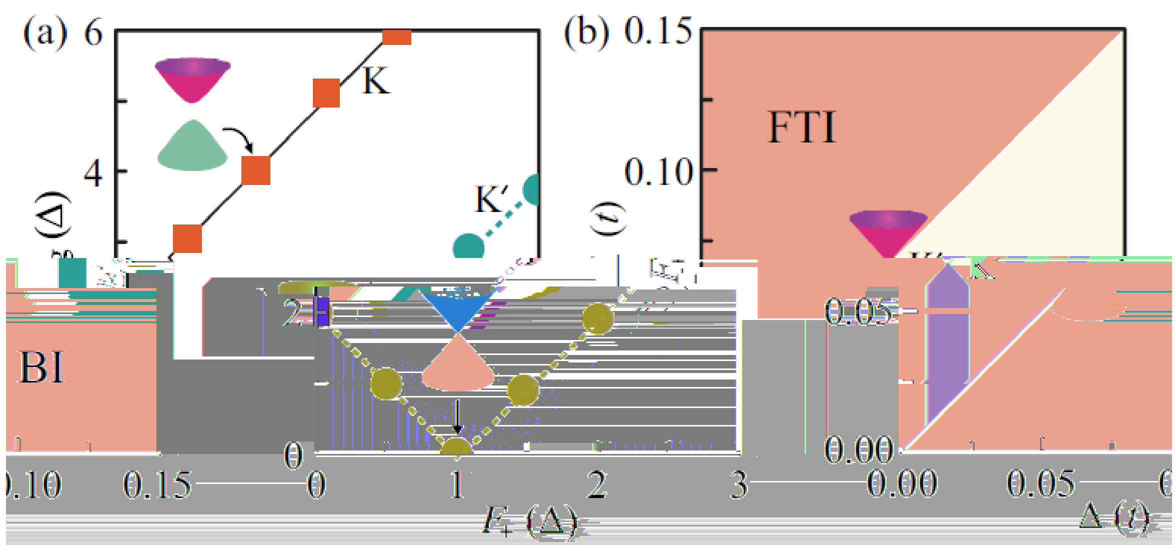

$$I = (eA\omega)^2/(8\pi\alpha)$$

3. Results and Discussion：

Berry

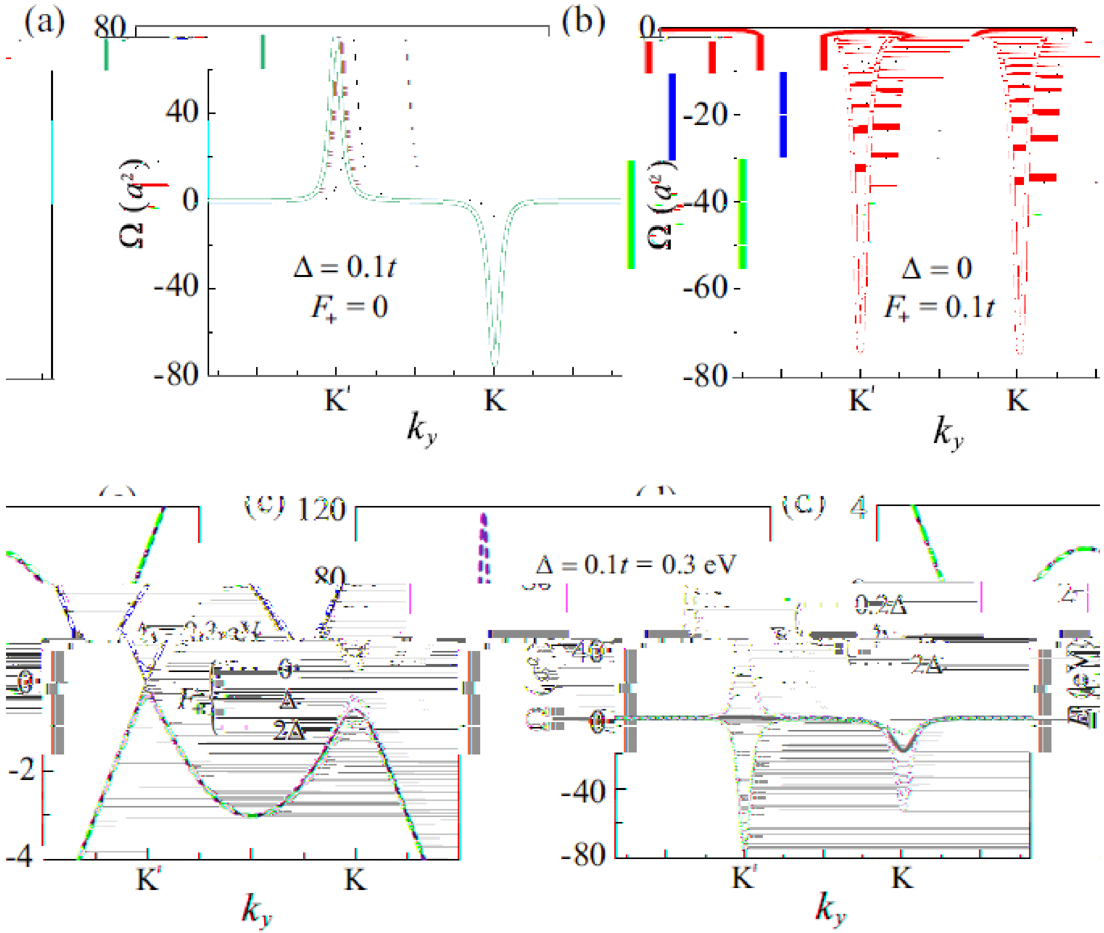

$$\Omega_-(\boldsymbol{k}) = -\frac{(\hbar v_F)^2(\xi\Delta + F_\eta)}{2[(\Delta + \xi F_\eta)^2 + (\hbar v_F k)^2]^{3/2}}$$

$$\Omega_+(\boldsymbol{k}) = -\Omega_-(\boldsymbol{k})$$

Floquet Chern

=0, ±1

3. Results and Discussion：

(BI) Floquet (FTI)

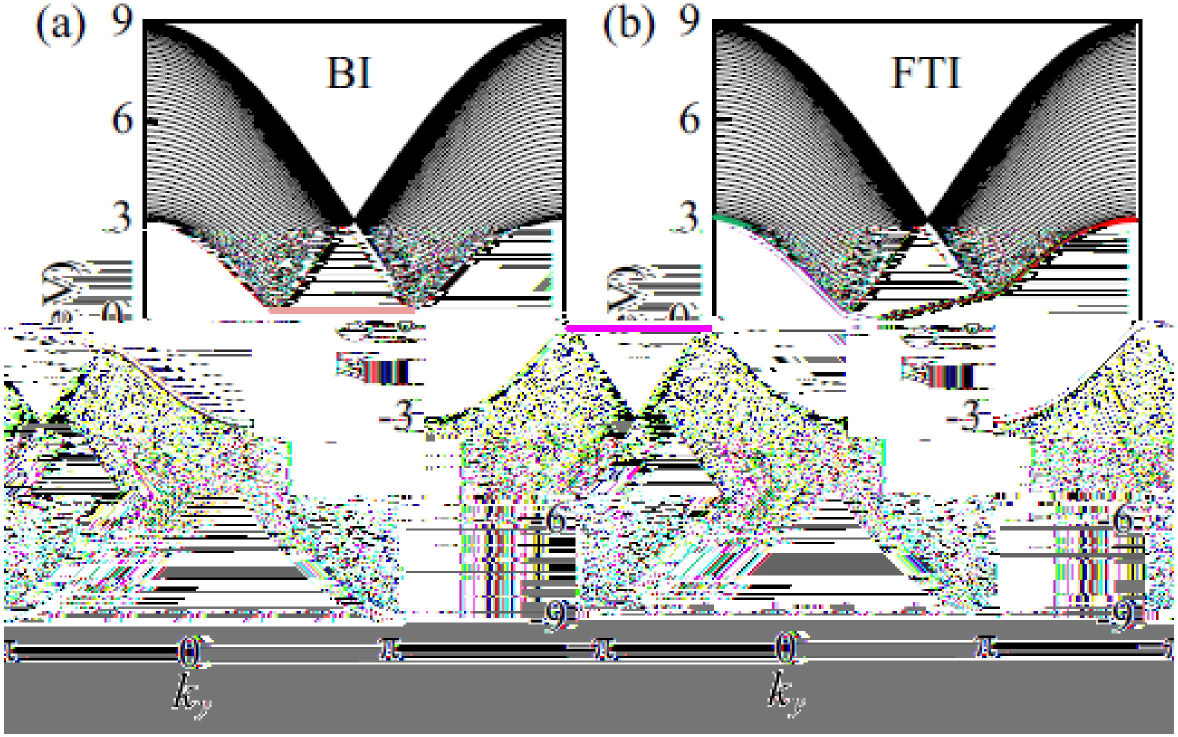

Band structure of a zigzag edged graphene nanoribbon with width 10 nm. (a) F_+=0, Δ=0.1t; (b) F_+=0.15t, Δ=0.1t.

3. Results and Discussion：

底 1 np

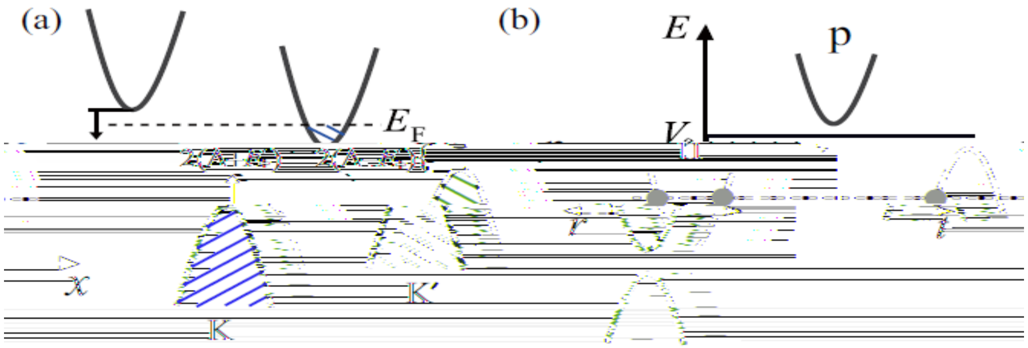

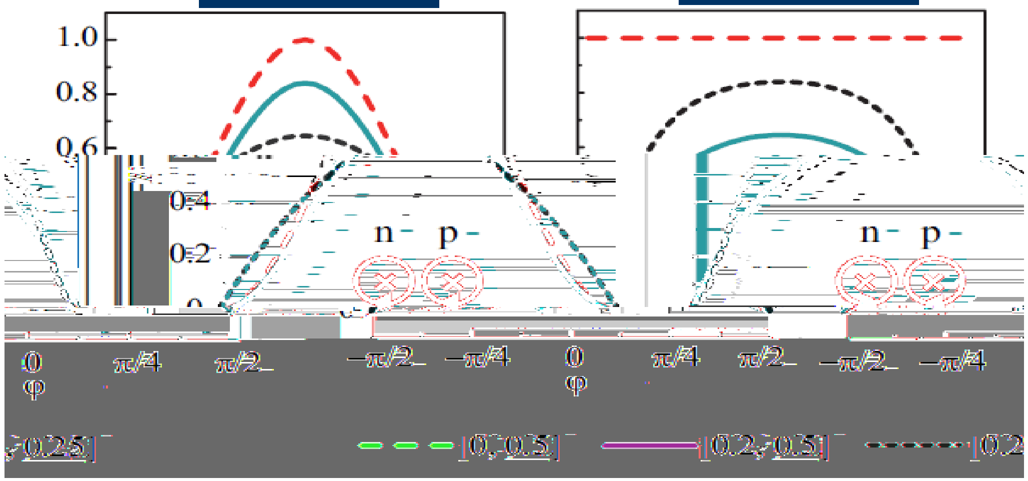

$[(\Delta - F_+)/V_0, E/V_0]$

Landauer-Büttiker formula

$$G = G_0 \int_0^{\pi/2} d\varphi T(\varphi) \cos \varphi$$

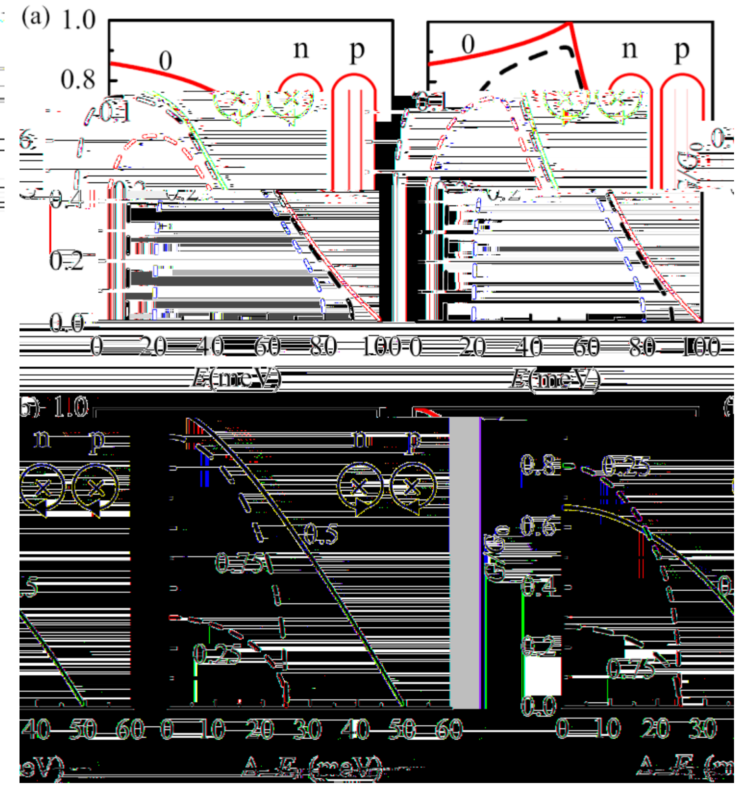

3. Results and Discussion：

底 2 底

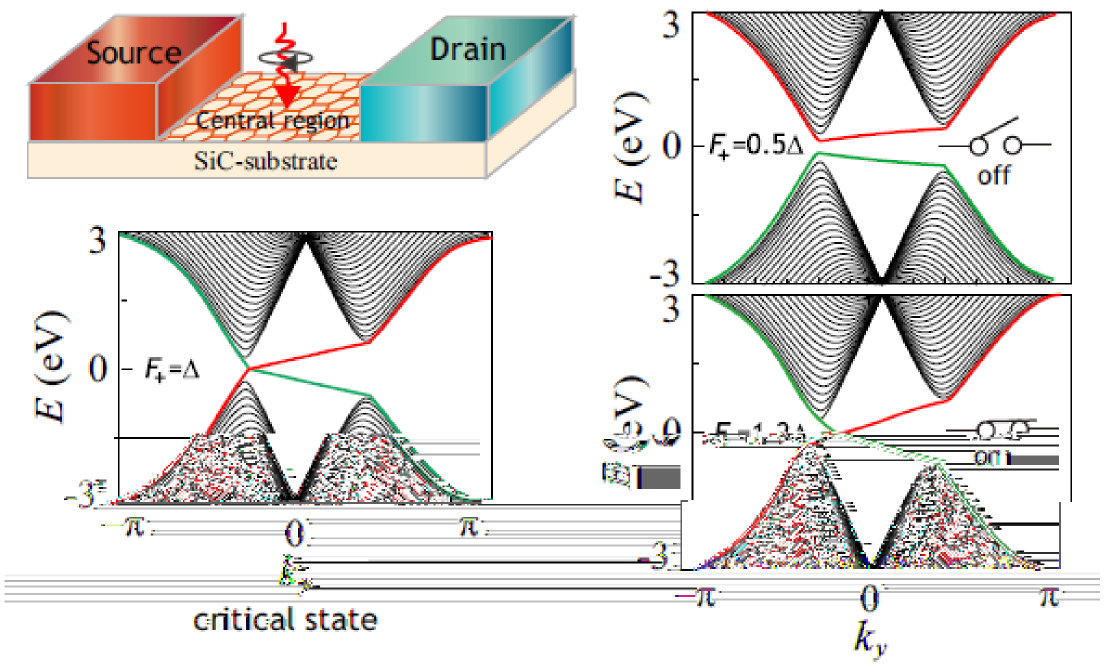

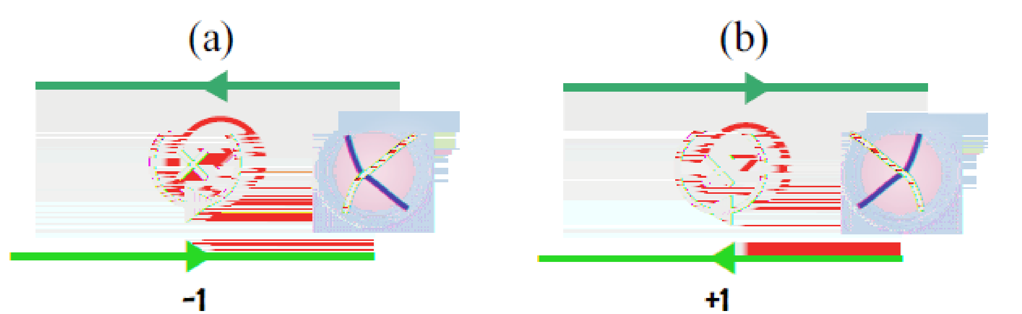

3. Results and Discussion;

底 3 底

The same setup for a graphene monolayer, irradiated by an off-resonance circularly polarized light, on a SiC substrate

$$E(\sigma_z, \tau_z) = (\Delta + \tau_z \Delta_\omega)\sigma_z$$

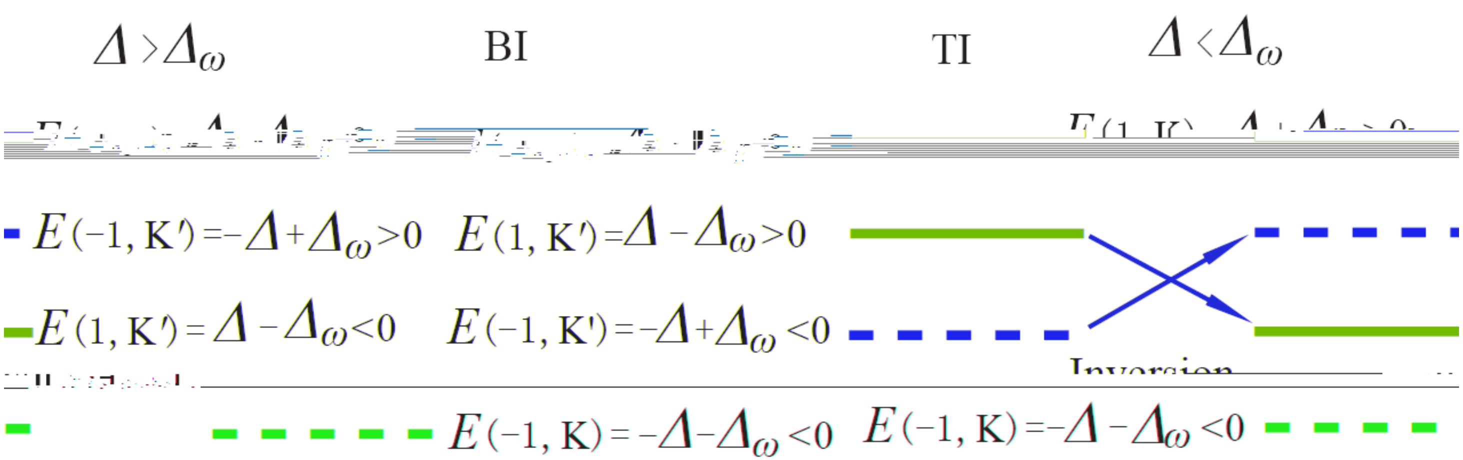

Band inversion. The blue solid (red dashed) lines represent conduction (valence) band in band insulating phase.

Nernst coefficient

$$\alpha_{xy}^{\tau_z} = \frac{2e}{\hbar T}\sum_n\int\frac{d\boldsymbol{k}}{(2\pi)^2}\Omega_n^{\tau_z}\left[(E_n - E_{\rm F})f + k_{\rm B}T\ln\left(1+e^{-\frac{E_n-E_{\rm F}}{k_{\rm B}T}}\right)\right]$$

Valley-dependent Nernst coefficient and the total Nernst coefficient versus Fermi energy. (a) In the BI phase (= 0.12 eV); (b) in the TI phase (= 0.14 eV).

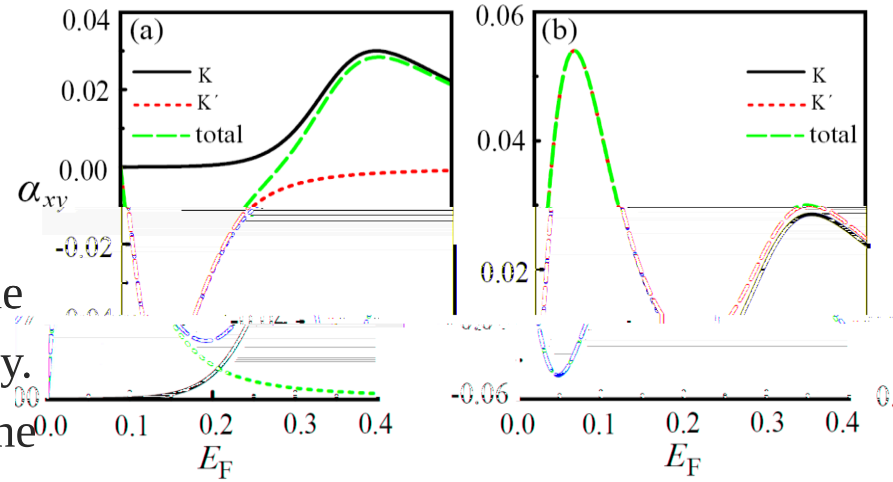

$$\alpha_{xy}^{\tau_z} = \frac{\pi^2}{3}\frac{k_{\rm B}^2 T e}{h}\frac{\tau_z\Delta + \Delta_\omega}{E_{\rm F}^2}$$

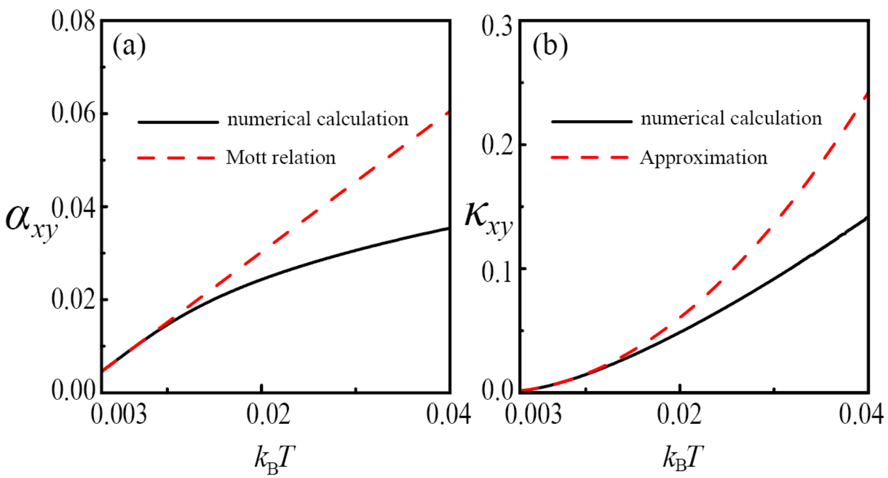

Ettingshausen coefficient

$$\kappa_{xy}^{\tau_z} = T\alpha_{xy}^{\tau_z} = \frac{\pi^2}{3}\frac{k_{\rm B}^2 T^2 e}{h}\frac{\tau_z\Delta + \Delta_\omega}{E_{\rm F}^2}$$

Total Nernst coefficient (a) and total Ettingshausen coefficient (b) versus $k_{\rm B}T$ at the topological phase transition point with $E_{\rm F}$ = 0.3 eV.

Nernst-Ettingshausen Figure of merit

$$ZT = \frac{\alpha_{xy}^2 T}{\sigma\lambda} = \frac{2\pi\Delta_\omega^2 k_B^2 T^2 h}{3\tau(\Delta_\omega E_{\rm F}^4 + 2E_{\rm F}^5)}$$

4. Summary: Some conclusions

Graphene-Like Two-Dimensional Materials

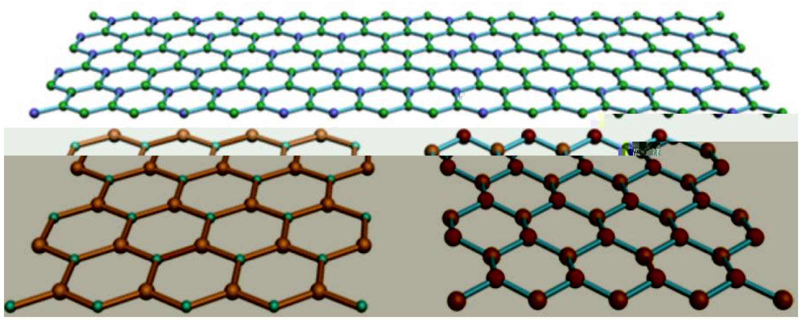

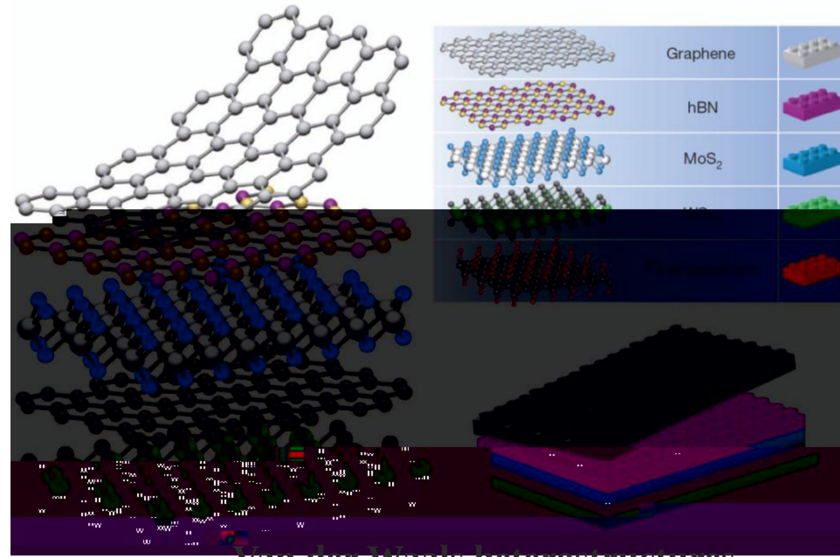

Van der Waals heterostructures

A. K. Geim & I. V. Grigorieva, Nature 499, 419 (2013).

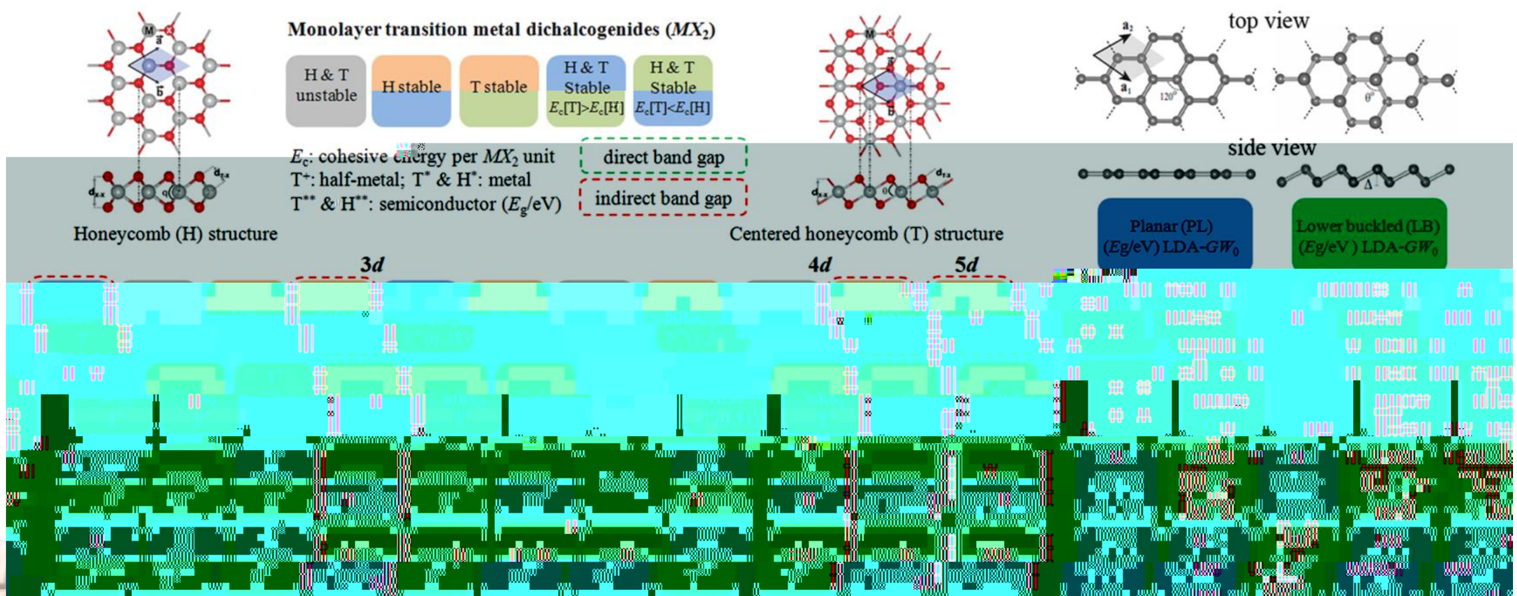

M. Xu, T. Liang, M. Shi, and H. Chen, Chem. Rev. 113, 3766 (2013).

Transport through graphene quantumdots

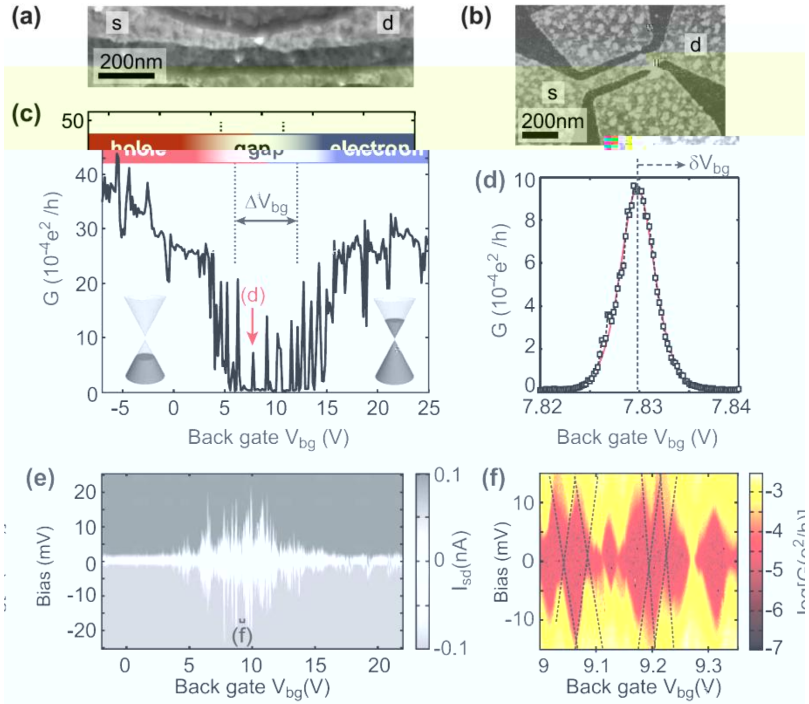

J. Guttinger et al., Rep. Prog. Phys. 75, 126502 (2012).

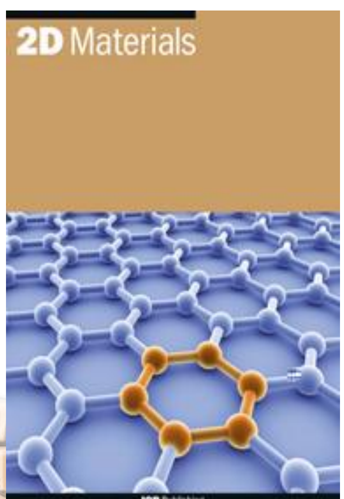

Vladimir Fal'ko
Editor-in-Chief
2D Materials

Two-dimensional flexible nanoelectronics

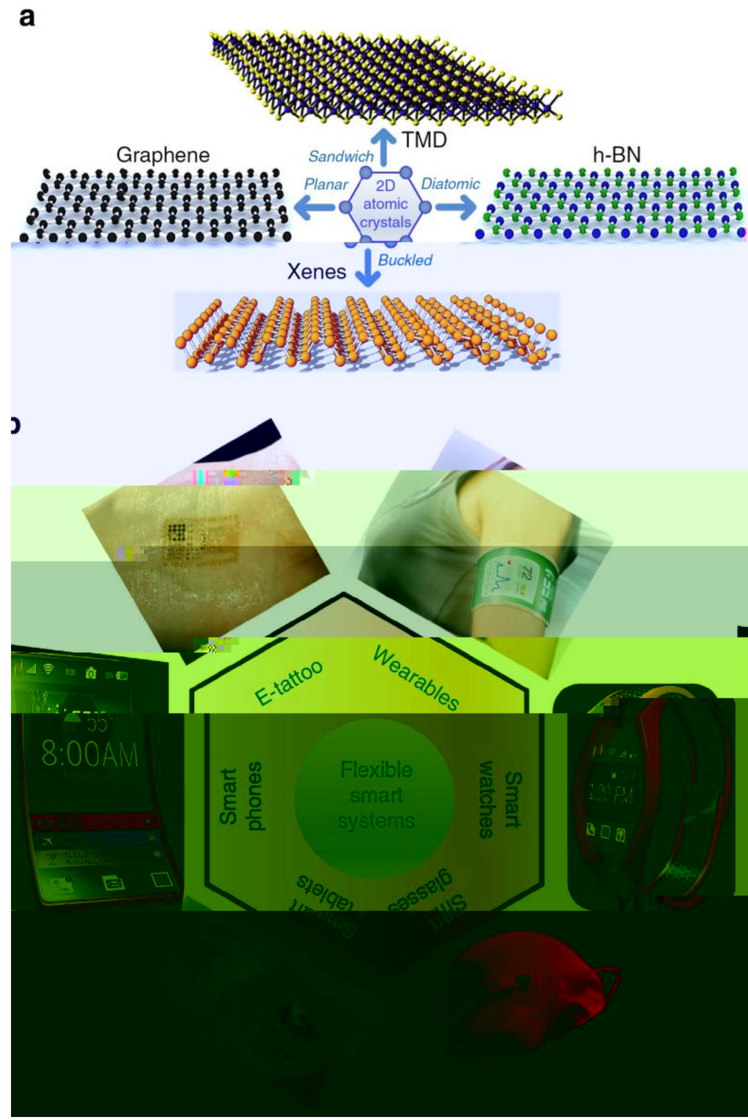

Akinwand, Petrone & Hone, Nat. Commun. 5, 5678 (2014).

, , , , 图 , 35, 1 (2015).

NATURE NANOTECHNOLOGY | VOL 10 | MAY 2015 | www.nature.com/naturenanotechnology

editorial

Graphene opens up to new applications

ffective separation membranes could be created by etching nanometre-sized pores in wo-dimensional materials.

he explosion of research interest i

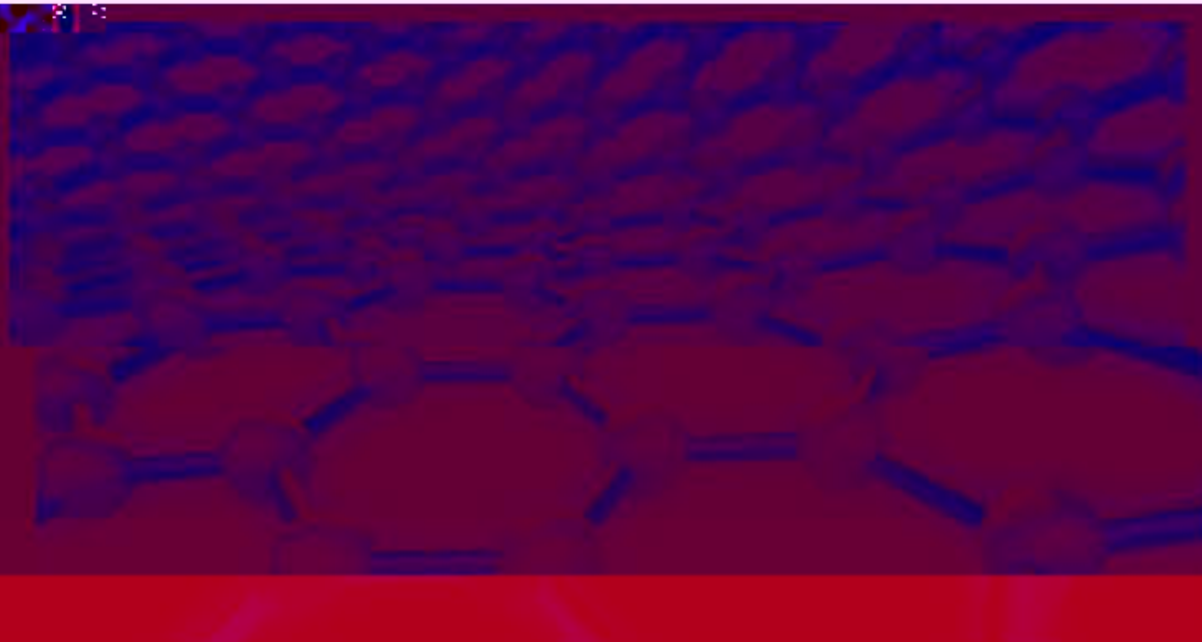

NATURE MATERIALS | VOL 14 | APRIL 2015 | www.nature.com/naturematerials

editorial

Physics gets its hands dirty

Is condensed-matter physics becoming more materials-oriented? Or is this just a new wrinkle in an old tradition?

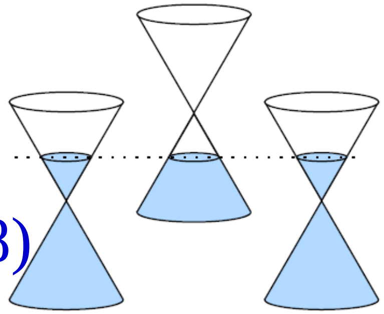

图 (2011CB922102),

左 (PAPD) 图 (11074108)